Applied Surface Science Advances 18 (2023) 100513

Contents lists available at ScienceDirect

Applied Surface Science Advances

journal homepage: www.sciencedirect.com/journal/applied-surface-science-advances

Advances in laser-based surface texturing for developing antifouling surfaces: A comprehensive review

Abhijit Cholkar [a,b,c,d,*], Ronan McCann [a,e], Gopinath Perumal [a,b,c], Suman Chatterjee [a,b,d], Mark Swayne [a,b,c], David Kinahan [a,b,d], Dermot Brabazon [a,b,c,d]

[a] I-Form, Advanced Manufacturing Research Centre, Dublin City University, Glasnevin, Dublin 9, Ireland
[b] Advanced Processing Technology Research Centre, School of Mechanical and Manufacturing Engineering, Dublin City University, Glasnevin, Dublin 9, Ireland
[c] National Centre for Plasma Science and Technology (NCPST), Dublin City University, Glasnevin, Dublin 9, Ireland
[d] DCU Water Institute, Dublin City University, Glasnevin, Dublin 9, Ireland
[e] Department of Science, School of Science and Computing, South East Technological University, Cork Road, Waterford City, Ireland

ARTICLE INFO

Keywords:
Antifouling surfaces
Femtosecond laser texturing
Nano-scale texture
Micro-scale texture
2D materials
Marine
Aerospace

ABSTRACT

Surface fouling is a major challenge faced within various engineering applications, especially in marine, aerospace, water treatment, food and beverage, and the energy generation sectors. This can be prevented or reduced in various ways by creating artificial surface textures which have fouling resistance properties. Ultrafast laser texturing provides an efficient method for the texturing of surfaces of different materials with high accuracy, precision, and repeatability. Laser texturing methods can enhance the production of well-defined surface nano- and microscale patterns. These surfaces with nano- and micro-scale patterning can be tailored to have inherent properties such as hydrophobicity, hydrophilicity, and resistance to fouling. This review gives an overview of the various types of fouling that can occur, the properties affecting a surface's fouling resistance, as well as the latest physical and chemical strategies for the generation of antifouling surfaces. Surfaces architectures which have inherent antifouling capabilities are presented. This review focuses on the utilization of the higher precision laser-based texturing offered from femtosecond laser systems for enhance fouling resistance. The process parameters to fabricate these textures and the current state of art femtosecond laser sources are presented and discussed. The challenges and future research requirements in the field of laser-based methods to fabricate antifouling surfaces are presented.

1. Introduction

Surface fouling is a phenomenon that occurs in many industrial applications and negatively impacts the performance of engineering components and systems. It is characterized by the accumulation of unwanted materials on a solid surface due to adhesion between the fouling material and the surface. It mainly occurs in applications in fields such as marine [1–4], aerospace [5–8], energy sector [9–12], medical [13–16], pharmaceutical [17] and food industries [18–21].

In recent years, there has been an increasing interest in developing anti-fouling surfaces, and researchers have been exploring various techniques to modify engineered surfaces and create functional surfaces that exhibit anti-fouling properties. It can be clearly seen from the "Scopus data" plotted below that there has been an increasing number of published works related to the topic of anti-fouling surfaces and using novel surface modification techniques such as laser texturing which shows the increasing interest of researchers and industries, see Fig. 1.

The history of anti-fouling surfaces dates back to ancient times, when the Phoenician civilization used copper and lead coatings to coat wooden boats. With the expansion of industrialization and transportation in the late 19th and early 20th centuries, there was significant research on developing anti-fouling surface strategies [22,23].

In recent decades, lasers have been used to modify surfaces with specific functionalities. Laser technology has advanced at a rapid pace, and the Nobel Prize-winning development of chirped pulse amplification technique [24] has enabled higher-power ultrashort laser pulses to be produced using less complex optics. This technology has resulted in the development of tabletop femtosecond laser systems. These can be used to modify surfaces without creating heat-affected zones and their associated defects. In recent times, there has been a surge of interest in

* Corresponding author.
E-mail address: abhijit.cholkar2@mail.dcu.ie (A. Cholkar).

https://doi.org/10.1016/j.apsadv.2023.100513
Received 31 May 2023; Received in revised form 16 November 2023; Accepted 16 November 2023
Available online 22 November 2023

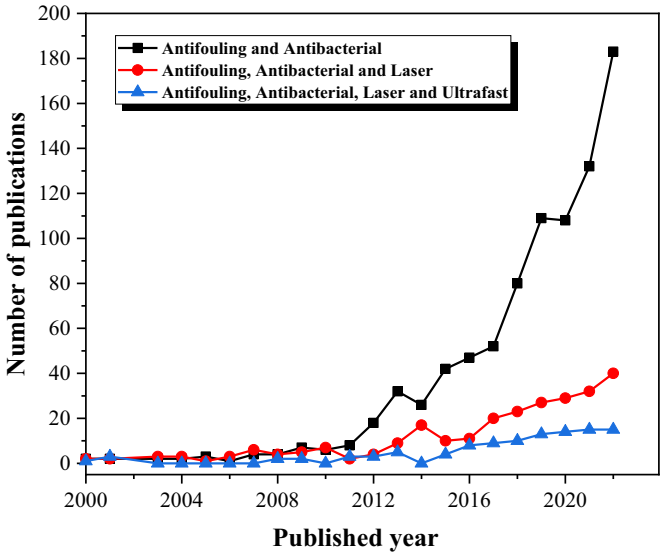

Fig. 1. Number of published articles indexed in Scopus on the topic of (a) antifouling AND antibacterial surfaces, (b) antifouling AND antibacterial surfaces with lasers, and (c) antifouling AND antibacterial surfaces with ultrafast lasers from 2000 to 2022.

GHz burst ultrafast lasers, owing to their remarkable ability to lower the processing threshold across a wide spectrum of materials while introducing novel nonlinear phenomena with significantly reduced heat effects and overall energy consumption [25].Femtosecond laser texturing has been widely applied in the development of micro/nanostructures and particularly to the manufacture of the super-hydrophobic surfaces that play a crucial role in many anti-fouling applications [26]. Recent research includes production of slippery liquid-infused porous surface (SLIPS) using femtosecond laser that could resist corrosion [27] along with self-healing properties [28]. However, production of these surfaces is more expensive, complex and they fail over the time due to the lubrication depletion, [29] degradation or poor stability of the lubricant layer [30].

Many attempts have been made to manufacture hydrophobic surfaces using laser texturing that play a very important role in many applications, such as anti-biofouling, anti-corrosion, and anti-icing surfaces [31]. The ability to fabricate biomimetic surfaces with precise control over their wetting properties presents a plethora of opportunities for various applications, such as developing self-cleaning surfaces that exhibit antifouling characteristics, improving the efficacy of oil-water separation, and enhancing the performance of green energy systems like batteries and fuel cells [32] (Fig. 2).

In addition, antibacterial and antifouling are distinct characteristics. Antibacterial is the ability to stop bacteria from growing and reproducing, whereas anti-fouling is the ability to stop unwanted substances

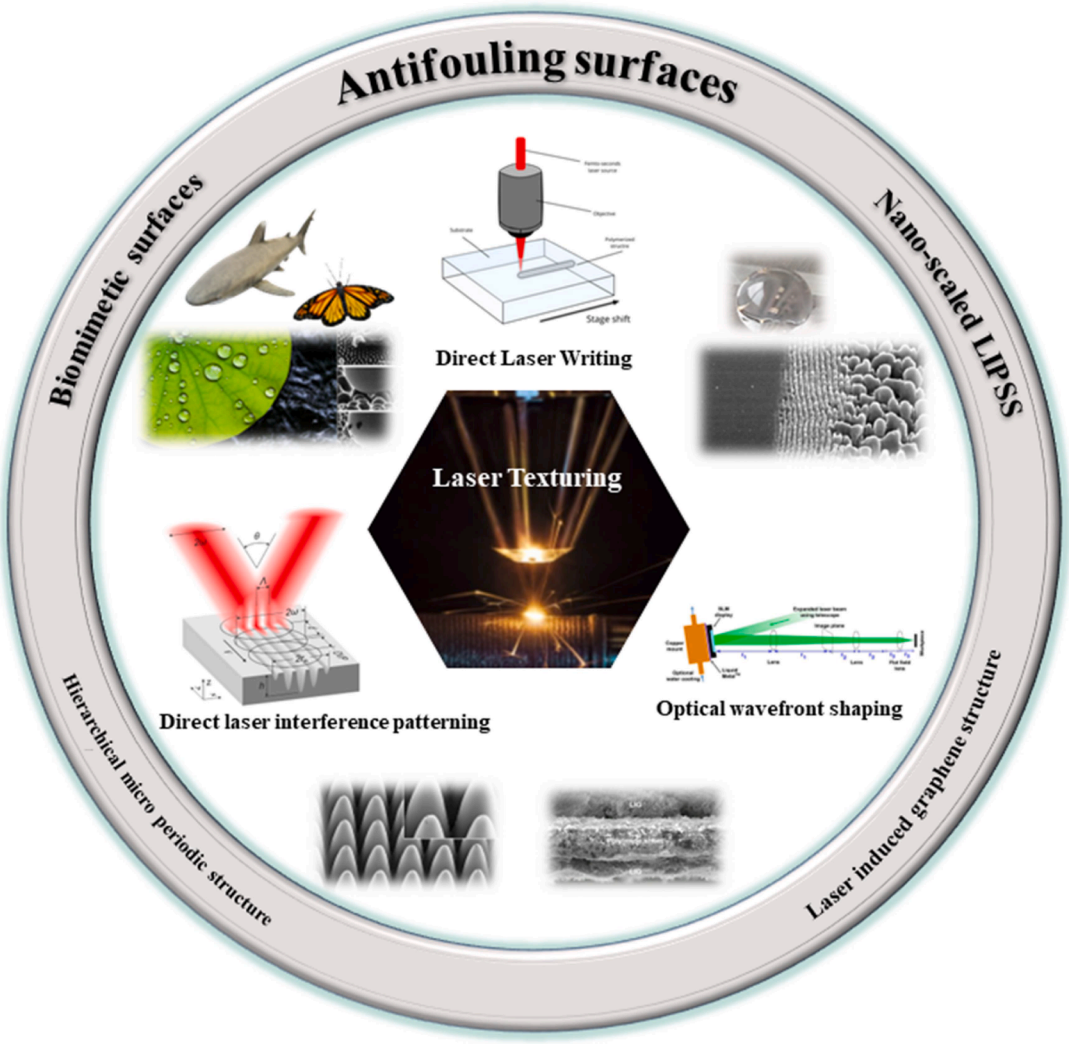

Fig. 2. Schematic of laser texturing strategies used to generate antifouling surfaces.

from adhering to a surface. Antibacterial coatings have ingredients in them that can kill bacteria or deter them from growing. On the other hand, anti-fouling coatings, are made to stop things like dirt, dust, and other contaminants from attaching to and accumulating up on a surface. However, in this paper, our focus is on anti-fouling surfaces produced by laser texturing.

The review paper begins with an overview of surface fouling and traditional anti-fouling methods. The mechanisms of surface fouling and how traditional methods such as coatings and surface modifications work to prevent or reduce fouling are presented. The various laser-based processing techniques and principles of laser-induced micro/nano texturing and how they can be used to control the wettability and corrosion rate of surfaces are discussed in detail. An overview of biomimetic micro/nanostructured surfaces and their potential applications in self-cleaning surfaces, oil-water separation, and green energy systems such as fuel cells and batteries are also presented. The challenges and limitations of the current surface texturing methods and the potential for future advancements in this field are discussed. The paper presents a summary and discussion of the current state of research and the future directions for developing anti-fouling functional surfaces using laser texturing techniques.

This review paper aims to provide a comprehensive overview of the use of ultrafast lasers for developing anti-fouling functional surfaces. It highlights the potential applications of these surfaces and the challenges and limitations of the current methods. This review will be useful for researchers in the fields of surface science, materials science, engineering, and physics, as well as in the marine, aerospace, energy, medical, pharmaceutical, and food sectors.

1.1. Surface fouling mechanisms

Fouling is a time dependant, complex, and undesirable process with diverse mechanisms depending on the type of surface and foulant involved. Foulants can comprise macromolecules, bacteria, and/or suspended particles, and can be stationary or moving [2]. The types of fouling can be primarily classified in two categories: microfouling (<100 mm) and macrofouling (>100 mm). Another type of categorisation used is illustrated in the Fig. 3.

There are six mechanisms of fouling, these are: 1. colloidal, 2. scale, 3. chemical, 4. corrosion, 5. biofouling and 6. ice [33,34]. Colloidal fouling, type 1, is a type of fouling that can be generated by organic or inorganic colloids. Fine particles with a size range of 1–1000 nm are involved. These colloids build up on membrane surfaces, reducing their performance. Fouling of this type is particularly common in reverse osmosis water filtration membranes. Aluminium silicate minerals, silica, iron oxides/hydroxides, and elemental sulphur are amongst the inorganic foulants found within various water sources [35].

Another important type of fouling is scaling, type 2, is caused by inorganic salts and other particles in the fluid stream. This type of fouling increases the pressure drop in a heat exchanger and lowers the heat transfer between the fluid and the heat exchanger surface. Settling of the salts can occur with the fluid flow velocity falls below a critical level. This type of fouling occurs in heat exchangers of heating, ventilation, and air conditioning systems, and is one of the leading causes of system failure and inefficiency [36]. The foulants or scales are made up of calcium carbonate or calcium sulphate precipitations which are insoluble in fluids such as water. This type of fouling is also known as precipitation, crystallization, or sedimentation fouling [37].

Chemical fouling, type 3 is a fouling type whereby solid is deposited on a surface due to a chemical reaction. A common form of chemical fouling is the formation of asphaltenes as a fouling species in crude petroleum streams caused due to the oxidative condensation process [38]. When there is a lack of oxygen at high temperature it results in the formation of coke which has a high molecular mass. There are various parameters which affect the formation such as the temperature, velocity of the stream, composition of the feedstock, autoxidation, polymerization, and thermal decomposition, presence of oxygen, presence of sulphur and nitrogen and other impurities in the stream, material of the surface and presence of inorganic components and other environmental factors. These factors affect the rate of the chemical reactions taking place and hence also the magnitude of deposit formation [39].

In type 4, corrosion fouling, a chemical or electrochemical reaction occurs between the surface and its environment. The anode and the cathode are connected electrically both through the fluid and by some external metallic conductor [40]. Charge is transported by the electrons due to current flow in the external conductor and by the ionized species in the fluid. On removal from the fluid and drying, the metal hydroxide loses its constituent fluid, and the remaining deposit consists of metal oxides. At the cathode, a electrochemical reaction occurs involving the reduction of oxygen dissolved in the fluid. These oxides and hydroxides

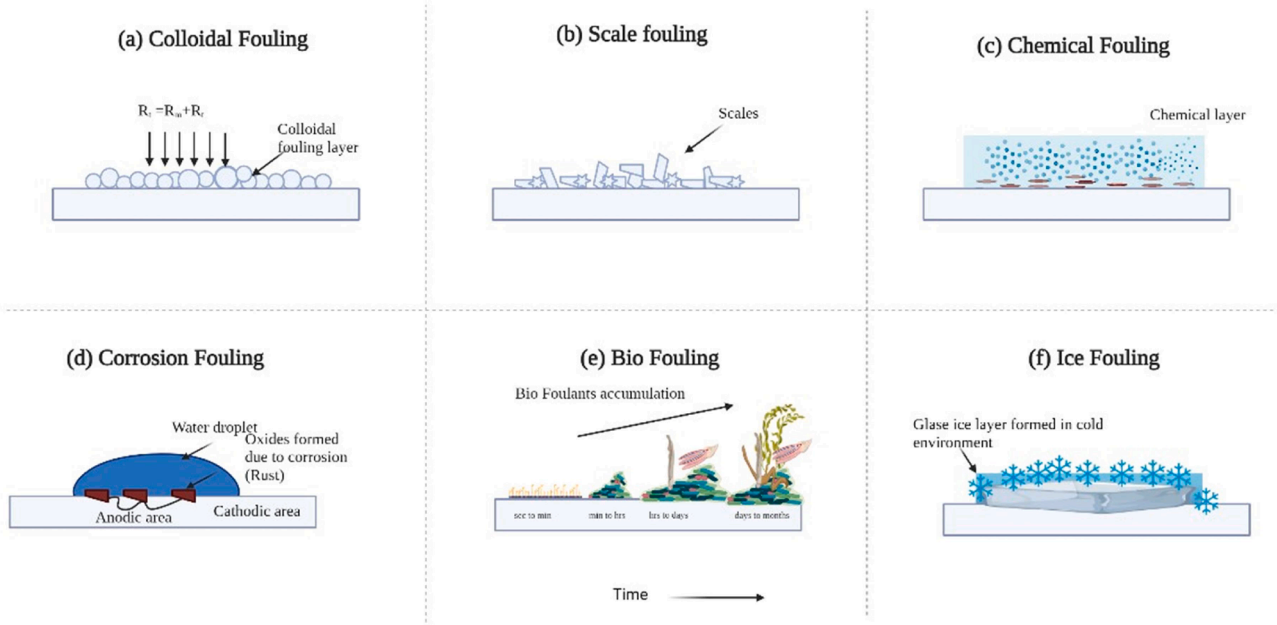

Fig. 3. Schematics of the fouling processes of (a) colloidal, (b) scale, (c) chemical, (d) corrosion, (e) biological species and (f) ice formation.

constitute the fouling deposit [41]. This type of fouling occurs with time in applications such as marine applications including ships hulls, propellers and other parts of ships or boats which come in contact with sea water [42]. When corrosion is accelerated directly by the life activities of microorganisms or indirectly by their metabolites, it is termed as microbiologically influenced corrosion [43], and occurs in heat exchangers such as steam boilers, condensers and in the food industry [44].

Biofouling, type 5 refers to undesirable attachment of microorganisms at a phase transition interface (solid–liquid, gas–liquid or liquid–liquid), which might occur due to deposition, growth and metabolism of bacteria cells or flocs on the surface [45]. Biological fouling takes place in various stages such as surface conditioning by formation of a conditioning film, attachment of pioneer planktonic cells onto surfaces, formation of microcolonies by primary bio adhesion and subsequently development of mature biofilms which destroys the interaction of the surfaces with the fluids or other surfaces. It occurs due to diverse array of fouling organisms and has increased operational expenses and deleterious impacts however the extent of information on its causes is still lacking. Various organisms responsible for biofouling especially in medical and marine environments along with the size of the bio foulants are illustrated below in Fig. 4.

Other organic foulants include polysaccharides, proteins, and natural organic matter [47]. Fouling from such species especially occurs in low and high-pressure membranes which are used in bioreactors [48]. The economic costs associated with biofouling control have been estimated to range from $1.5 to 3 billion per year [49]. The reduction of biofouling on the propeller and hull of a ship can significantly increase the resistance of the ship flow through the water [50].

Ice fouling, type 6, is one of the significant types of fouling in which ice is formed and accumulates on surfaces due to the low temperature and low pressure environmental conditions [51]. This occurs especially on aeroplane wings [52], power lines, wind turbines [9] and heat exchangers in cooling systems used in the food industry [53] due to the solidification of the fluids which come in contact with the surface at low temperature and pressure. Ice nucleation and growth which contaminates the surfaces, reduces the functional efficiency of these systems [33].

As fouling has been a problem for long time and directly affects the performance of many engineered systems, there is a need to develop surface manufacturing methods such that fouling can be prevented. The below sections introduces the surface characteristics that affect the anti-fouling performance.

1.2. *Surface properties affecting fouling resistance*

There are various properties which are linked to the fouling resistance of a surface. The most important properties affecting the fouling resistance are listed below.

Surface texture: The texture of a surface can affect fouling resistance. A smooth surface tends to be less prone to fouling, while a rough surface provides more places for fouling agents to attach. The best condition is to achieve control over the surface roughness [54].

Material composition: The composition of a material affects its fouling resistance. For example, some materials are naturally resistant to fouling, while others are more susceptible to it [55].

Surface energy: The surface energy of a material affects its ability to repel or attract fouling agents. Materials with higher surface energy tend to be less prone to fouling because they repel unwanted substances. The surface energy is calculated by measuring the contact angle of the surface which determines the wetting behaviour. The schematic diagram shown in Fig. 5 helps to feature the four different wetting behaviour of the surface such as super-hydrophilic, hydrophilic, hydrophobic and super-hydrophobic nature of the surfaces. When water contact angle is less than 10° the surface is called as superhydrophilic; when the contact angle is less than 90° the surface is called as hydrophilic; when the contact angle is more than 90° the surface is called as hydrophobic; and when contact angle is more than 150° the surface is called as superhydrophobic [56–60].

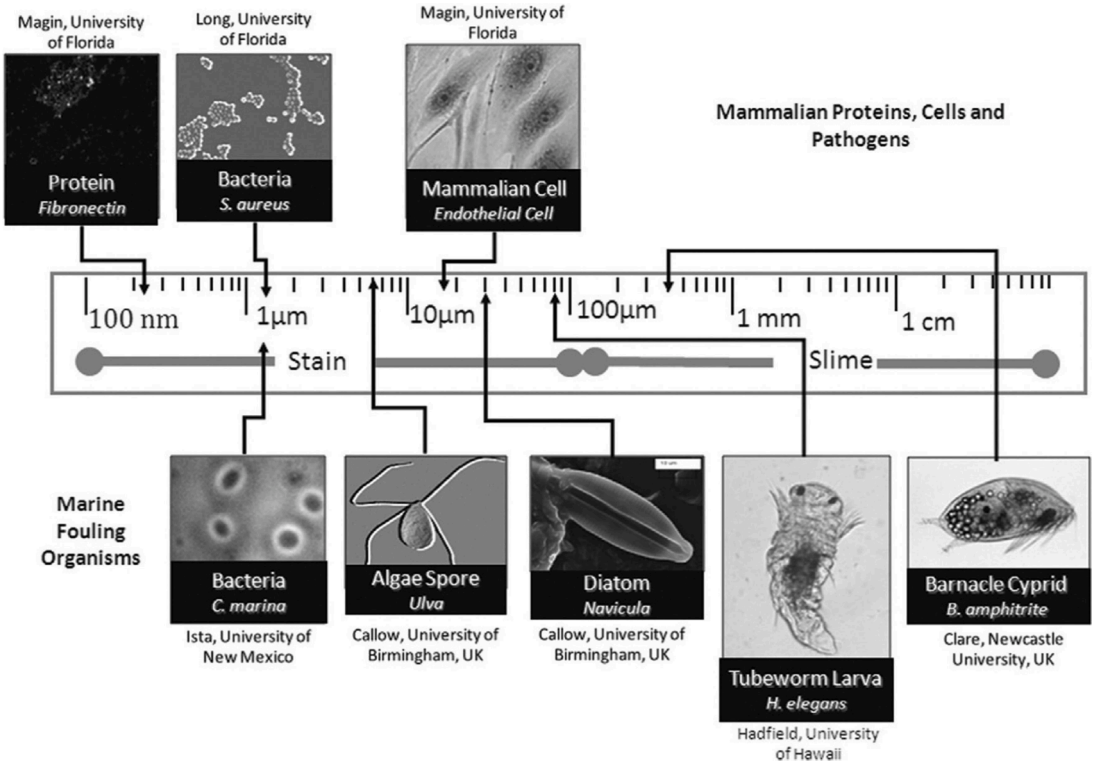

Fig. 4. Illustration of different bio-foulants found in biomedical and marine environments. Cells and compounds relevant to biomedical applications are shown above the scale axis. Marine organisms are shown below the scale. Reproduced with permission from [46].

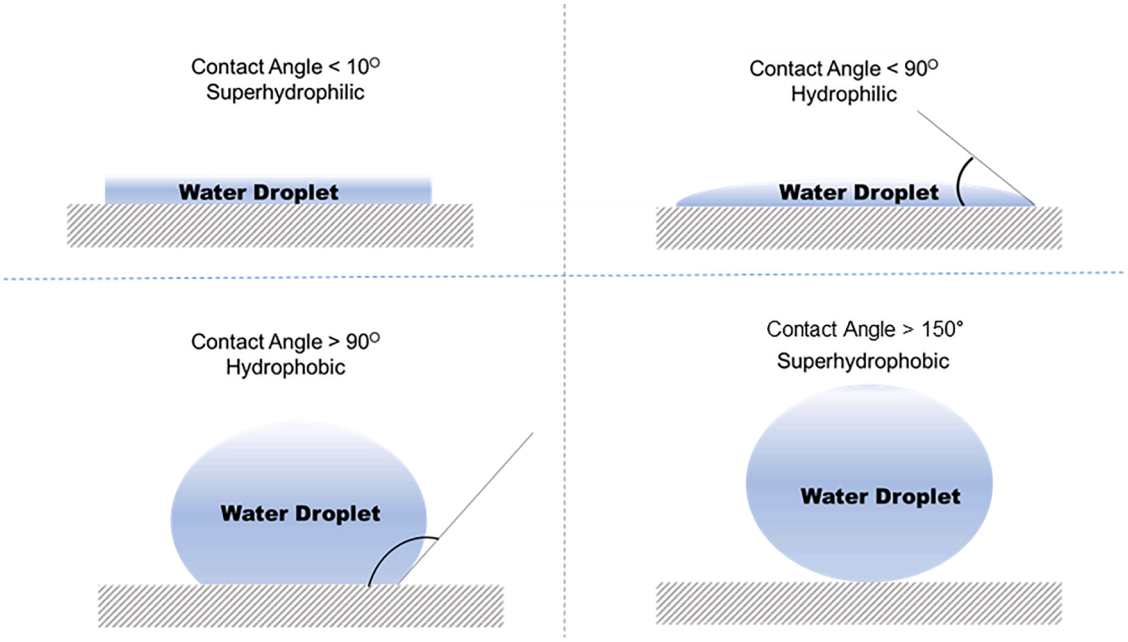

Fig. 5. Schematic of four different wetting behaviour on the surface of the substrate.

1.3. *Characterization of surface fouling properties*

In general, there exist numerous techniques to evaluate the fouling properties of surfaces. The majority of fouling characterisation methods employ self-made laboratory experiments that are tailored to the specific application of the material . At first, a significant number of works measure the hydrophobicity and icing characteristics of newly developed metal surfaces using contact angle measurements. Contact Angle Hysteresis (CAH) was utilized to measure wetting phenomena and fluid-metallic surface interactions [61]. Furthermore, the phenomenon of freezing effect or ice adhesion is commonly evaluated by the experimental arrangement depicted in the Fig. 6(a)–(c). The calculations involved determining the icing delay time and the contact interaction time in relation to the anti-icing or freezing qualities of the surface. In order to assess the strength of ice adhesion, many methods were employed, including the peak force method, centrifugal force method, tensile force method [62].

In general, biocorrosion was characterized using the conventional

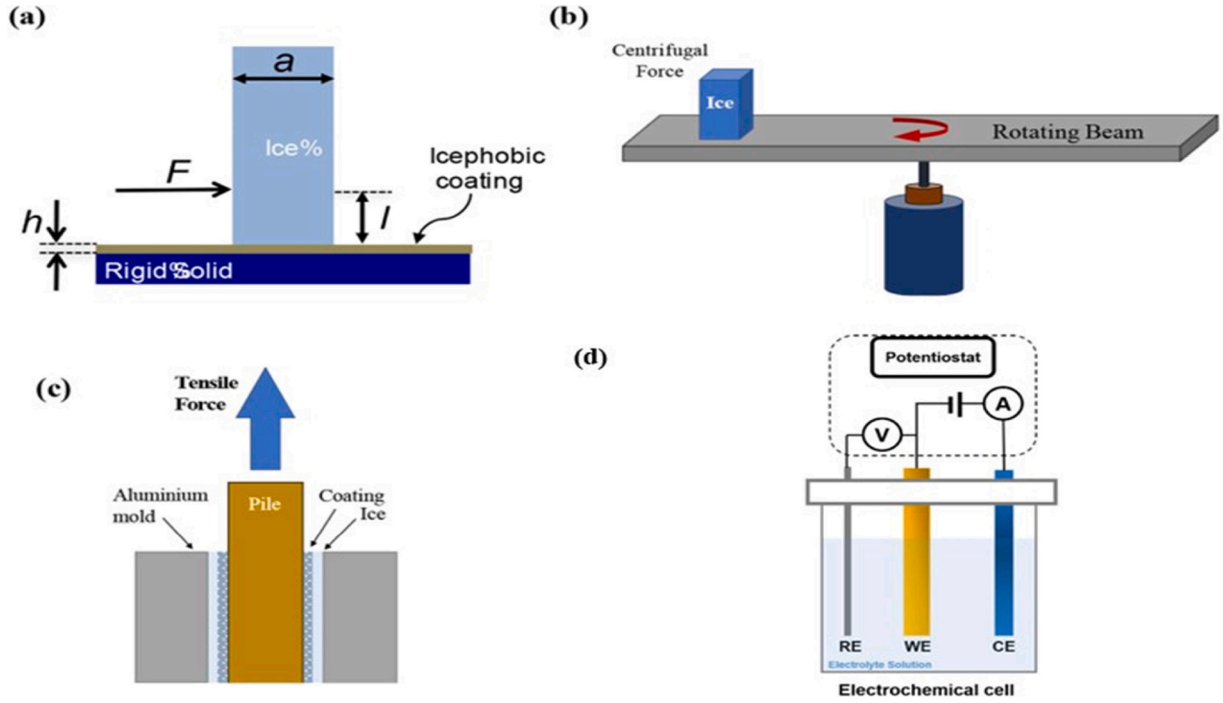

Fig. 6. Illustrations of experimental methodologies used to assess ice adhesion (a) Cuvette-encased ice column: This approach involves measuring the shear stress required to detach an ice column that is encased in a cuvette from the surface; (b) Centrifugal force method: In this method, induced shear stress at the ice-coating interface is measured by subjecting the system to centrifugal forces; (c) Tensile force method: This technique utilizes a tensile machine to induce shear stress at the interface, evaluating the adhesion of ice to the coating; (d) 3 electrode electrochemical setup to test corrosion Reproduced with permission [64,62].

method of weight loss and electrochemical characterization. Electrochemical characterization consists of tests such as open circuit potential (OCP), Potentio-dynamic polarization (PDP), and linear polarization experiments utilizing a three-electrode setup shown in Fig. 6(d). Electrochemical impedance spectroscopy (EIS) and Mott-Schottky (MS) studies were also used to passivation or oxide layer on the metallic surface [63]. These approaches were utilized to quantify the ice adhesion strength which evaluates the anti-freezing capability of the metallic surface. Few common in-vitro methods for biological assays include growth inhibition studies using absorbence measurements, colony forming unit (CFU) counting using ImageJ, live/dead bacteria staining tests using fluorescence microscopy, and morphological analysis using scanning electron microscopy (SEM). In summary, all these assays offer initial evaluations for the overall integrity of the prepared surfaces before applying their real-time utilization.

2. Different strategies of producing antifouling surfaces

2.1. Physical strategies

Anti-fouling surfaces have gained significant interest due to their potential applications in various industries. Physical approaches to prevent organism attachment involve designing surfaces with micro- or nano-scale textures, effectively deterring settlement. Lithographic techniques are frequently utilized for crafting intricately structured surfaces in this context. These approaches vary from the application of radiation to harden or soften photosensitive material, which is then removed via wet chemical approaches [65], imprint techniques utilising stamping for surface structuring, to beam lithographic approaches which rely on focused particle beams for material sputtering [66]. Conventional manufacturing approaches such as hot embossing and vacuum casting [67] have also been scaled to the nano- or micro-scale, and are suitable approaches for producing features for anti-fouling surfaces. Finally additive manufacturing approaches, often referred to as 3D printing, where parts can be fabricated in a layer wise manner, also offers the possibility for direct production of anti-fouling surface features [68]. Several physical-based methods have been proposed for the fabrication of anti-fouling surfaces, as summarized in Table 1.

The selection of a suitable manufacturing process is crucial for achieving high productivity, scalability, dimensional accuracy, extended lifetime, and low cost. These considerations are particularly important in the field of surface engineering, where the ability to produce features of a specific size range and material composition is essential. One approach for creating such surfaces is the use of hot embossing and imprinting techniques. Nevertheless, these approaches are limited in their applicability, as they can only be applied to a selected materials which are compatible with the process. Similarly, while lithography has the capacity to yield high-quality surface features, it involves high costs.

2.2. Need of laser surface processing

Laser surface texturing offer a promising and adaptable approach for manufacturing anti-fouling surfaces. This technique can process a wide range of materials and surface feature sizes, and the potential for high productivity and dimensional accuracy is significant. Additionally, laser texturing and machining is an innovative process that can also be used for large surface areas, making it an attractive option for applications such as marine coatings [112,113].

One of the primary advantages of laser texturing and machining is its versatility in material selection. The technique can be used with a broad range of materials, including metals, ceramics, and polymers. Additionally, this technique can produce features of various sizes, from microscale to macroscale, making it a flexible approach for creating surfaces with tailored functionalities [26,114,115].

Another significant advantage of laser texturing and machining is its

Table 1
Physical based methods for the fabrication of anti-fouling surfaces.

Method		Description	Refs.
Lithographic techniques	Photolithography	Uses light to transfer a geometric pattern from a photomask to a photosensitive chemical photoresist on the substrate.	[65, 69–75]
	Electron beam lithography	Scanning focused beam of electrons to draw on a surface covered with an electron-sensitive film called a resist. It is capable to produce high precision 3 to 5 nm patterns.	[76–81]
	Ion beam lithography	In this technique focused beam of ions in a patterned fashion across a surface to create very small structures.	[66,79,82]
	Soft lithography	It uses PDMS as master template and can produce micro and nano patterns.	[83–85]
	Nano-imprint lithography	Patterns are generated by mechanical deformation of imprint resist, cured by heat or UV light during the imprinting.	[86–90]
	Colloidal lithography	In this method the colloidal crystals are used as a masque on the surface of the substrate used.	[91–95]
Nano and Micro moulding		It is a fast fabrication method for transferring nanostructures on to a substrate made up of polymer. In this process a mould is created that has a cavity in the shape of the part desired.	[96,97]
Vacuum casting		In this method, a mould is placed onto a PDMS sample and is completely covered in unsaturated polyester resin which contain glass fibres under vacuum conditions. This method is commonly used to reproduce the patterns.	[67, 98–100]
Reactive Ion etching		In this process the plasma is initiated in the system by applying a strong radio frequency electromagnetic field to the wafer platter, the positive ions tend to drift toward the wafer platter, where they collide with the samples to be etched. The ions react chemically with the materials on the surface of the samples and remove material in nanoscale.	[101–105]
Hot embossing		Stamping of pattern into the polymer softened by increase in temperature above glass transition temperature.	[106–108]
Additive Manufacturing		Versatile and various micro or nano patterns can be manufactured using layer by layer addition of material.	[68, 109–111]

potential for high productivity and dimensional accuracy. The use of lasers allows for precise control over the surface modification process, resulting in high accuracy and consistency in feature size and shape. Additionally, the use of lasers enables the creation of complex geometries and patterns that would be challenging to achieve using other methods [116].

Several papers show extremely interesting surface patterns and effects when using GHz burst of fs pulses for surface modification, but in particular Obata et al. in 2022 [117] and Paschotta et al. in 2023 [118] that two dimensional LIPSS can be directly generated in this way, opening a new path for high productivity structuring of surfaces with superhydrophobic and self-cleaning effects.

Hence, laser texturing offers a compelling option for manufacturing anti-fouling surfaces. Its material adaptability, scalability, high productivity, and dimensional accuracy make it a promising approach for surface engineering.

3. Ultrafast laser texturing

The earliest report on the application of short and ultrashort lasers in materials processing dates back to the early 1980s [119]. The development of chirped pulse amplification technique in 1985 to produce high energy ultrashort pulse width pulses has enabled the development of ultrashort pulse laser systems such as the femtosecond laser which has advantages such as delivering high energy density at spatial and temporal scales of femtosecond lasers [24]. The first publication of the femtosecond laser being used was reported in 1991 [120]. This laser has proven its capability to be used in a number of laser micro/ nano machining applications, including biomedicine, photonics, and semiconductors. In these lasers it is possible to change the states and properties of materials through the interaction with them and they can be used to control materials for processing from micron to nanometre scales. Hence the femtosecond lasers can process almost any material with high quality and high precision and realize three-dimensional complex structure fabrication [121]. The general setup of femtosecond laser is as illustrated in Fig. 7.

By employing laser structuring, it becomes feasible to fabricate a variety of artificial surfaces that undergo topography alteration through thermal ablation patterning. This particular technique has the ability to fabricate micro or nano scale topologies on the surface. Another approach, known as patterning by optical interference, has the capacity to produce laser-induced periodic surface structures (LIPSS) that serve as artificial wavelength-scale surface formations. Additionally, patterning through surface hydrodynamic effects entails the creation of spikes as well as the imitation of natural surfaces, resulting in the formation of artificial nanoscale hills and valleys. This process serves to enhance the hydrophobic or hydrophilic properties of the given surface. Furthermore, laser ablation is employed to modify the microstructure of the material. This involves processes such as amorphization and crystallization as well as the formation of novel phases, including the processing of thin film shape memory alloys like nitinol. In certain instances, femtosecond laser surface structuring is also capable of simultaneous modification of topology and microstructure. [123].

3.1. Ultrafast laser-matter interaction

Pulsed laser systems are classified into two types based on their pulse duration: short pulse laser systems, which operate in the microsecond and nanosecond range, and ultra-short laser systems, which operate in the picosecond and femtosecond range [124]. The industrial term "ultrafast lasers" refers to laser systems that emit ultrashort pulses with pulse durations ranging from 100 femtoseconds to 100 picoseconds. These laser systems typically have pulse repetition rates in the megahertz or gigahertz range [119].

The interaction between pulsed lasers and materials can be categorized into three groups, as depicted in Fig. 8. The initial ultrafast processes occur due to electronic excitation (yellow) resulting from nonlinear multiphoton absorption processes. Energy transfer from excited electrons to atomic vibrations (green) takes place within picosecond ranges. Nonlinear photoionization processes, such as multiphoton or tunnelling, dominate the absorption of ultrashort laser pulses with durations of tens of femtoseconds (fs). Material ablation occurs in three steps within the femtosecond to picosecond range, as indicated in the yellow boxes in Fig. 8. First, the absorption of light due to inverse Bremsstrahlung occurs in the outer layer. Next, the electron thermal wave propagates through fast energy relaxation within the electron subsystem. Finally, electron-lattice relaxation occurs due to electron-phonon coupling [114].

However, in short pulse lasers the material interaction is different. Fig. 8 (turquoise), represents the formation of melt pool which forms heat affected zones after solifications which occurs due to absorption of laser energy, generally in short pulse lasers such as nano second laser.

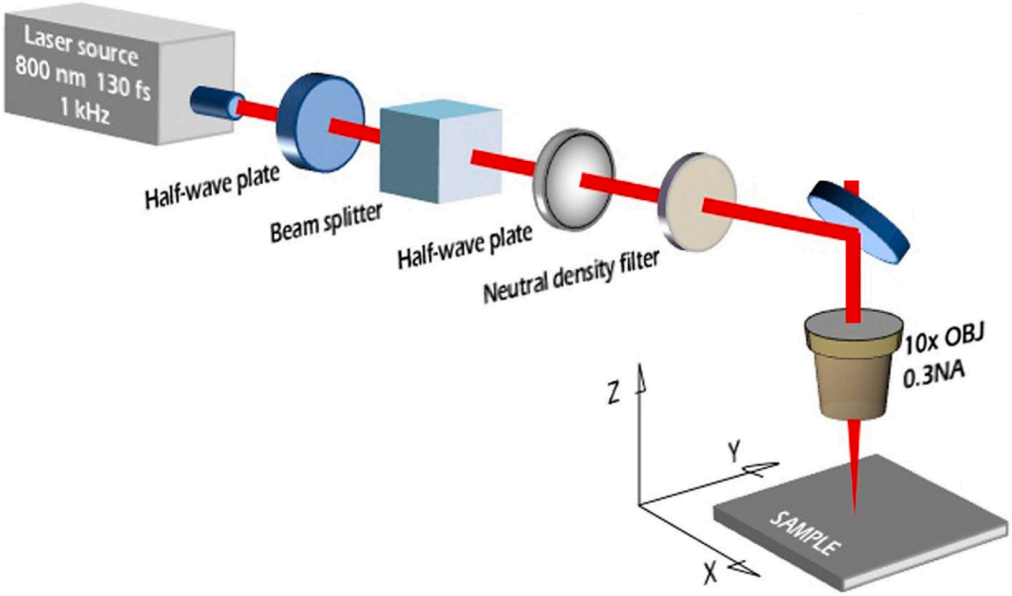

Fig. 7. Typical ultrafast laser texturing setup; Reproduced with permission [122].

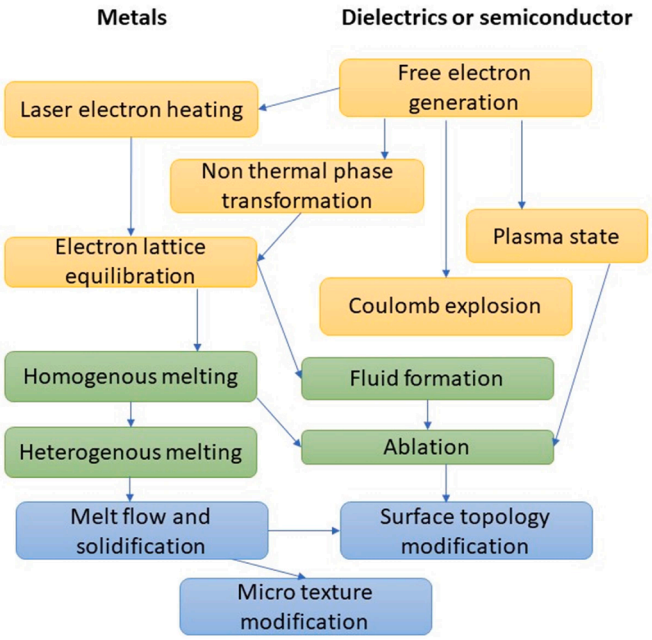

Fig. 8. Energy dissipation and phase transformations following the excitation of a material by an ultrashort laser pulse.

The heat, which is conducted in form of heat flux, melted, evaporated, or formed into plasma in the material depending on the temperature reached. The ablation mechanism depends on pulse duration and pulse energy.

The wavelength of the laser light holds significant influence over the absorptivity of various materials. Moreover, it has an impact on the depth of cut, machining capability, and the quality of surface features produced [125]. Fig. 9 shows the effect of wavelength on the absorptivity of different materials such as aluminium, gold, silver, copper, molybdenum, iron, and steel. In this way the laser matter interaction depends on the wavelength and the pulse duration.

3.2. Key process parameters in ultrafast laser texturing

The key process parameters in ultrafast laser texturing include laser pulse duration, laser fluence, repetition rate, and scanning speed.

Laser fluence is defined as the amount of energy delivered per unit area of the target material. It is a critical parameter because it determines the extent of material removal and the formation of a specific microstructure on the processed surface. The optimal laser fluence depends on the physical and chemical properties of the target material [127].

Repetition rate is another important process parameter in ultrafast laser texturing. It refers to the number of laser pulses delivered per unit time. High repetition rates result in a higher processing speed, but they also increase the likelihood of heat accumulation and thermal damage in the processed material [127].

Scanning speed is the speed at which the laser beam is moved across the target material. It determines the overlap of successive laser pulses and influences the quality of the processed surface. Slow scanning speeds lead to a higher level of precision and accuracy, while higher scanning speeds result in higher processing speeds [128].

Overlap pattern plays a crucial role in laser texturing, a key parameter in achieving high-precision and high-resolution laser machining. To achieve a uniform ablation of the target material while following a specified path, it is essential to control the machining speed, which is directly tied to the degree of overlap between consecutive laser spots. The resulting texture is critically influenced by the temporal and spatial separation between successive laser pulses, a factor determined by the laser repetition rate and the chosen scanning strategy. It can be written in following form [129–131].

$$O_v = \left(1 - \frac{v}{2w.\,PRR}\right) \times 100$$

Laser pulse duration is the time taken by a laser pulse to complete a

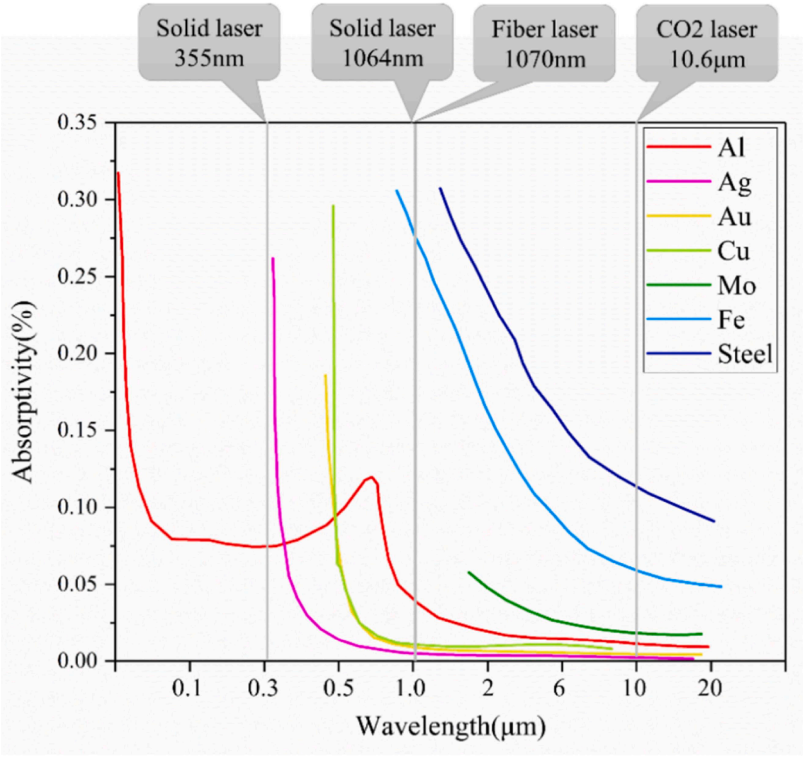

Fig. 9. Absorptivity of metals with respect to wavelength Reproduced with permission [126].

single cycle. It is one of the most critical process parameters in ultrafast laser texturing because it determines the peak power and energy density of the laser pulse. Shorter pulse durations result in higher peak powers and energy densities, leading to enhanced material removal rates and improved quality of processed surfaces. This is because long and short laser pulses in the range of millisecond to nanosecond pulse lengths are described by thermal ablation which is dominated by heat conduction, melting, evaporation, and plasma formation. If the pulse length is longer than the relaxation time the energy absorbed by the material is conducted away from the source as heat, this will produce a temperature field in the work piece known as the heat affected zone (HAZ). This will produce a melt pool around the heat source application location [132]. The extreme pressure and temperatures caused by the ultra-short pulse build up and accelerate the ionized material to extremely high velocities. Due to the short timescale continuous evaporation of the material does not occur, instead the material is transferred into an overheated liquid state. This high pressure overheated liquid merges into a mixture of vapour and liquid droplets causing a rapid expansion of the material removing it from the ablated area [133]. The femtosecond laser texturing is named as cold processing as the laser power appears off before electrons transferring energy to lattice. The size of the HAZ can vary widely based on the material and process parameters, and in some cases, it can extend well beyond 10 nm.. A comparison of the ablation by long pulse such as micro or nanosecond width and ultrashort pulse width lasers such as femtosecond laser is shown in Fig. 10.

Other laser process parameters, such as polarization, beam profile, and depth of focus, exert a considerable influence on the quality and characteristics of the resulting textures, as well as their dimensional accuracy and thus, the overall quality of the topology. In the study under consideration, the laser fluence was manipulated, and the process of laser polishing was executed on titanium alloy. The obtained results, specifically the SEM analysis and surface roughness measurements, revealed that an increase in laser fluence leads to a corresponding increase in the variability of surface roughness [135].

3.3. Material processing using ultrafast laser machining

A significant body of research has been conducted on the application of laser texturing to various materials, including metals, polymers, ceramics, and semiconductor materials. The resulting textures and features, as well as the surface antifouling capabilities, have been analysed in depth and are summarized in the accompanying Table 2. The choice of laser type and the specific material being textured play a crucial role in determining the resulting surface characteristics. These findings contribute to the growing body of knowledge on the use of laser texturing as a viable technique for enhancing the properties of various materials.

3.4. State of art laser-based nano- and micro-scale surface modification techniques

Three important ultrafast laser-based material processing techniques which appear in the literature and are used to manufacture antifouling surfaces are direct laser writing (DLW), direct laser interference patterning (DLIP) with a microscopic objective or galvoscanner, and Optical Wavefront Shaping (OWS). The main differences between them lie in their principles of operation, precision, scalability, and specific applications.

3.4.1. Direct laser writing

Direct laser writing (DLW) is one of the most common laser texturing techniques that has been shown to be effective in generating antifouling properties on surfaces. An example of the setup for DLW is shown in Fig. 11. The relative ease of DLW processing and simpler equipment compared to other techniques is well noted [151]. DLW has been used to produce a plethora of different 3D micro structure on a large variety of materials [152]. Even with its excellent texturing ability DLW is hindered by it low through-put processing minimizing its efficiency in large scale processing. To combat this issue DLW more recently be combined with the other laser texturing method such as LIPSS or DLIP.

In the study by Chu et al., he utilization of nanosecond direct laser writing (DLW) is employed to generate a microcellular pattern on TiAl6V4, which possesses a width of 50 μm. Subsequently, the implementation of picosecond Direct Laser Induced Periodic Surface Structures (DLIP) is employed to fabricate micropillars within the larger microcells, with a width of 2.6 μm. This process results in the creation of a hierarchical micro-nano structure on the material's surface, leading to an augmentation in the water contact angle (WCA) to a value exceeding 110° [153]. Also, DLW method to fabricating super hydrophobic steel surfaces using a two-step process of water confined laser texturing in combination with an immersion in chlorosilane solution to increase the hydrophobicity of the textured surface. Submerging the steel specimen in deionized water confines the laser pulse induced plasma, increasing the effect of the laser and allowing for a higher throughput. This process produces super hydrophobic micro-nano scale textures on the surface of the steel. The effect of different laser power on the final water specific

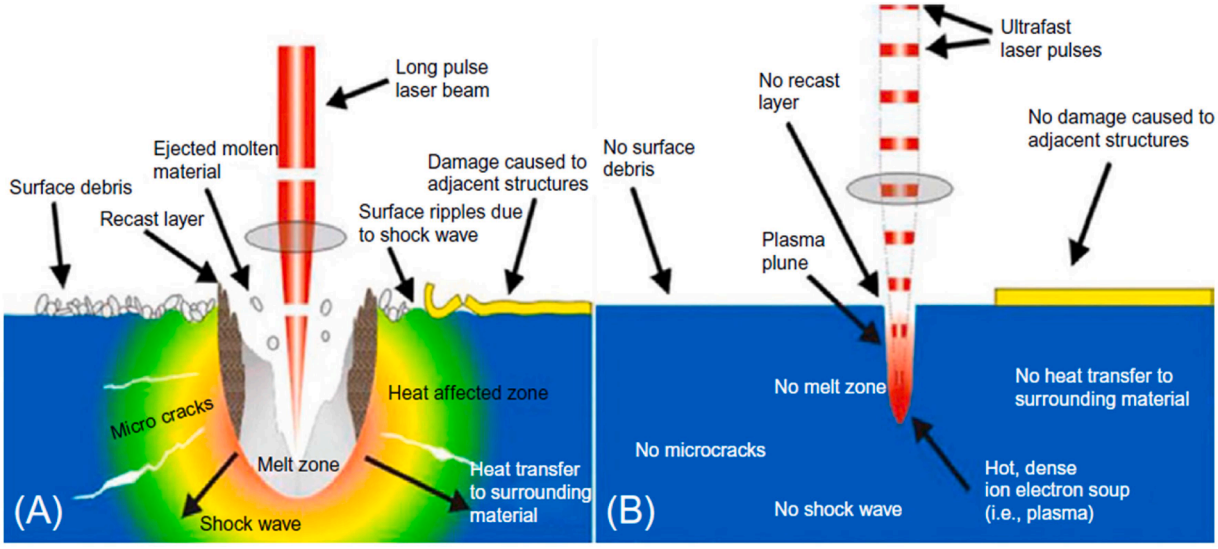

Fig. 10. (a) Long and (b) short pulse laser ablation. Reproduced with permission [134].

Table 2
List of laser and processes used for surface structuring suitable for the generation of anti-fouling surfaces.

Substrate Material	Laser Specification				Feature Size/Morphology	Notes	Refs./ Year
	Type	Wavelength	Pulse width	Pulse reptation rate			
Ti6Al4V	Nd: YVO_4	1064 nm	10 ps	103 kHz	Parallel lines with variable hatch distance. Sample Ti_1 was processed using laser parameters of 0.178 J/cm^2, 10 mm/s and 10 μm; Ti_2 with 0.138 J/cm^2, 1 mm/s and 10 μm and Ti_3 with 0.178 J/cm^2, 100 mm/s and 80 μm.	Antifouling characteristics were enhanced. However, this was combination of chemical and laser processing.	[136]
Titanium foam	Diode-pumped Yb	1030 nm	250 fs	75 kHz	line-by-line scan with 10 μm hatch distance	The oil water separation efficiency was improved drastically and oil fouling ability was improved. This is for the pristine Ti foam material.	[137]
Titanium (Ti6Al4V) and Stainless steel (100Cr6)	Ti: sapphire	790 nm	30 fs	1 kHz	Parallel lines	Tribological properties were enhanced	[138]
Titanium foil	Ti: sapphire	800 nm	50 fs	1KHz	Micro drilling of sizes 15 to 70 μm	Micro drilling was conducted on thin film. More precise holes need to be manufactured to enhance the performance. Using optical wavefront shaping could be one of solution to machine with high precision.	[139]
Steel alloy 40CrMnMoS8–6 (1.2312),	Ti: Sapphire with diode pumped Yb: KGW	1026 nm	170 fs	1 kHz	Line pattern of hatch distance 20 μm	The ammonia gas and laser structuring both have effects on hydrophobicity and corrosion resistance.	[140]
Austenitic stainless steel (AISI304)	Ti: Sapphire	800 nm	130 fs	1 kHz	Trench and matrix micropattern. LIPSS nano pattern with 30, 50 and 90 μm distances.	Single one-step femtosecond laser fabrication process. Controlled hydrophobicity is achieved.	[141]
Pure Gold	Ti: Sapphire	800 nm	30 fs	1 kHz	Conic and 1D-rod-like structures with hatch distance of 50 μm to 150 μm	Attempt was made to make antibacterial surface by converting hydrophobic to superhydrophobic surface. The randomly distributed nano/micro- structures have pockets where bacteria can form colonies. Hence these can be avoided by using precise laser systems.	[142]
Black platinum, titanium, and brass	Ti Sapphire	800 nm	65 fs	1 kHz	Parallel microgrooves covered by extensive nanostructures array	The superhydrophobic and self-cleaning anti reflective surface is manufactured using femtosecond laser on three different materials.	[143]
Zirconia Ceramics	Ti: Sapphire	800 nm	35 fs	2 kHz	Well-distributed periodic and cyclic microstructure of 50 μm	High quality-controlled topography at the micrometric and sub-micrometric scale is enabled using femtosecond laser on hard to machine zirconia ceramics	[144]
Polystyrene and Polydimethylsiloxane	KrF	515 nm	380 fs	200 kHz	Micro- and nano-sized structures with hatch distance range of 8–15 μm	PS was processed using UV laser and then two-step process in which steel mould is treated with laser and the nano structures are transferred to the polymer surface by hot embossing was conducted.	[145]
Polyethylene, polycarbonates, Polyethylene terephthalate, Polylactic acid, polymethyl methacrylate, and polytetrafluoroethylene	Ti: Sapphire	800 nm, 275 nm	85 fs	1 kHz	LIPSS were generated with 44 μm and 35 μm spot sizes.	Optical and chemical properties were observed	[146]
Poly (ethylene terephthalate), poly (trimethylene terephthalate) and poly carbonate bis-phenol A	Ti: sapphire	795 nm; 265 nm	120 fs	1 kHz	Laser induced periodic structures		[147]
Polytetrafluoroethylene	Ti: sapphire	800 nm,	85 fs	10 kHz	Fibrous surface structure	Non wetting properties of the laser processed area is investigated	[148]
Cyclic olefin polymer	Ti: sapphire	775 nm	150 fs	1 kHz	Microchannels with pitch was fixed at 0.02 mm	Superhydrophobic properties of the cyclic olefin polymer were investigated	[149]
Silicon (n-doped, (111)-orientated)	Ti: sapphire	800 nm,	56 fs	1 kHz	Micro-hole structures along with nano structures at the boundary	Combination of chemical and laser processing. Anti-reflective properties were attained using this technique.	[150]

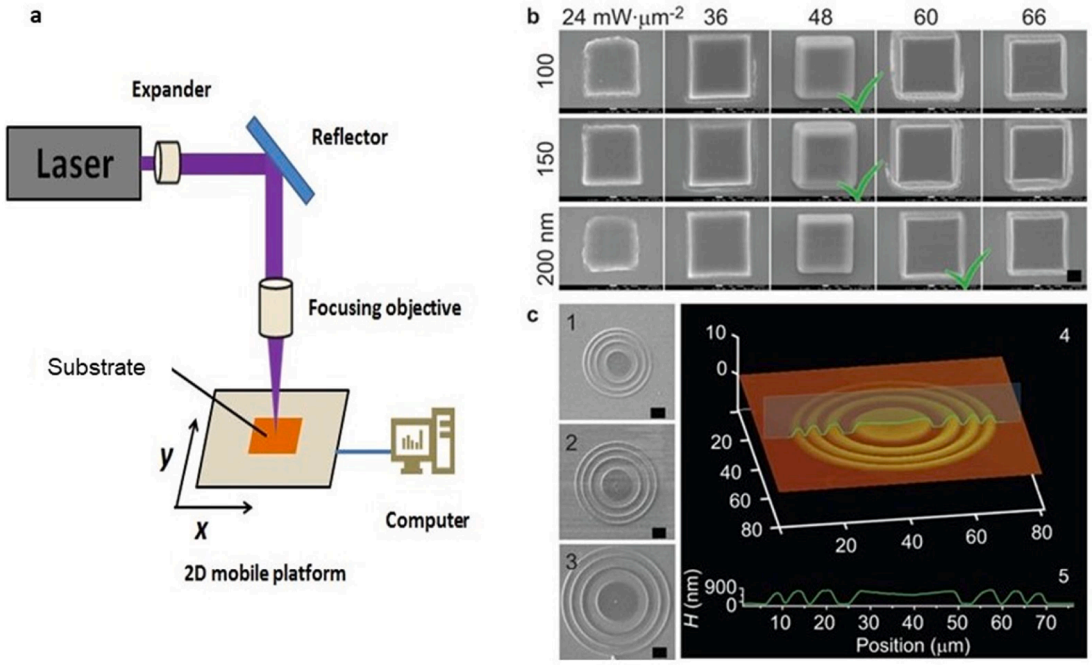

Fig. 11. (a) Direct laser writing process, (b) SEM images showing topography influenced, and (c) SEM images of glass cover slips and AFM characterization exhibiting 3D morphology. Reproduced with permission from [155].

contact angle (WSCA) was investigate and showed a sharp increase in WSCA from 0 to 0.2GW/cm^2 where the WSCA was 155° [154]. While DLW has demonstrated excellent texturing ability, its low throughput processing remains a significant limitation. The combination of DLW with other laser texturing methods shows promise in addressing this limitation. The use of DLW in conjunction with water confinement and a chlorosilane solution has also shown promise in producing super hydrophobic surfaces. Further investigation into the efficacy and scalability of these methods is needed to determine their practical applications in industry.

3.4.2. *Direct laser interference patterning*

Direct Laser Interference Patterning (DLIP) incorporates multiple overlapping laser beams to produce an interference pattern. This process produces periodic micro-nano structures on the surface of the material with the structures corresponding to the amplitude distribution of the interference pattern [156]. These textures have antifouling properties as the micro- and nano-scale features can interfere with the attachment of bacteria and other biological materials. The polarization, number of beams and laser fluence all contribute to the distribution and size of the final texture produced [157]. DLIP is a highly suitable approach for high throughput processing due to its ability to process sub-millimetre scale areas with a single pulse, and fast processing speeds of up to 0.9m^2/min as shown in the research by [158]. However DLIP has developed in recent times with development of 500 W and up to kW class ultrafast lasers, which allow for much larger spot sizes closer to 1 cm^2 [159–162]. LIPSS is also commonly formed during the DLIP process producing higher order structures on the surface [163]. The effect of altering process parameters on the homogeneity of DLIP processed structures on Ti6Al4V using a nanosecond Nd: YLF laser was investigated. The authors reported that hatching distance is the most significant parameter for the surface homogeneity. with a relevant importance on the large periodic modulation, it shows that the hatching distance must be a multiple of the interference spatial period and must be smaller than the laser beam diameter. Higher pulse to pulse overlaps also showed the highest texture homogeneity with the overlap having a strong influence on the structural depth of the line pattern. This increase homogeneity has been seen to increase the water contact angle and antifouling properties. Fig. 12 shows the working principle of the DLIP process. In the Fig. 12, ω is the beam diameter, Λ is laser intensity profile/ ablated structure period, θ is beams intersection angle, d is the distance between the laser spots, OVP is the spot overlap; v is the samples' translation speed; R_{oth} is the radius of ablated area and h is ablated structure depth [164].In a recent study by Schröder et al. and Ranke et al. high energy pulses without generating large thermal effects, so higher and higher laser powers and pulse energies are allowing larger processing spot sizes which changes the prospects of laser surface texturing dramatically, while generating 3D or complex shapes [159,165].

While DLIP offers promising results for a range of industrial applications, its limitations, and the impact of process parameters on the final surface texture must be carefully considered to ensure optimal results. Further research is needed to optimize the DLIP technique and improve its efficiency for large-scale processing.

3.4.3. *Optical wavefront shaping*

Optical wavefront shaping techniques have been developed to fabricate complex textures [168]. These techniques involve manipulating the amplitude and phase of light waves to achieve desired wavefronts. Various methods have been proposed to achieve wavefront shaping, static techniques such as spatial light modulators (SLMs) [169] see Fig. 13. and plasmonic gap waveguides [170]. And dynamic techniques such as digital micro-mirror devices (DMDs) have also been used for wavefront shaping, offering faster refresh rates compared to SLMs [171]. Additionally, wavefront shaping through multi-core fibers (MCFs) has been demonstrated, enabling precise intensity manipulation of the reconstructed light field [5]. Furthermore, a fabrication-free tunable flat slab has been developed using a nonlinear four-wave mixing process, allowing for the manipulation of light propagation in an all-optical manner . These advancements in optical wavefront shaping provide opportunities for creating complex textures. Each of the technique provides different flexibility, contrast, cost effectiveness or working area, thus each having a different optimal application field. It has been used to generate both functional and optical surfaces, surfaces for biological applications. The diffractive multi-beam patterns are

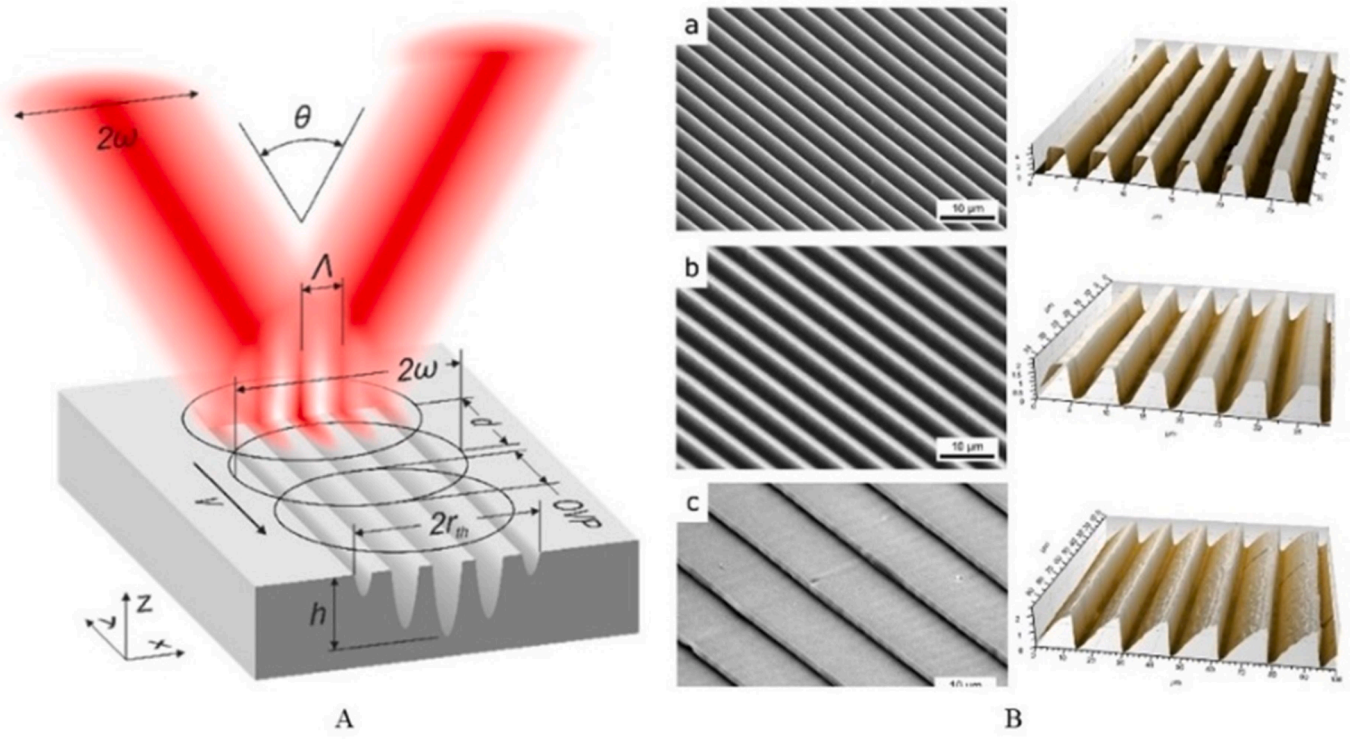

Fig. 12. A. Model of direct laser interference patterning (DLIP), B, SEM micrographs (left) and confocal topography (right) of the structured polyimide foils using DLIPS Reproduced with permission from [166,167].

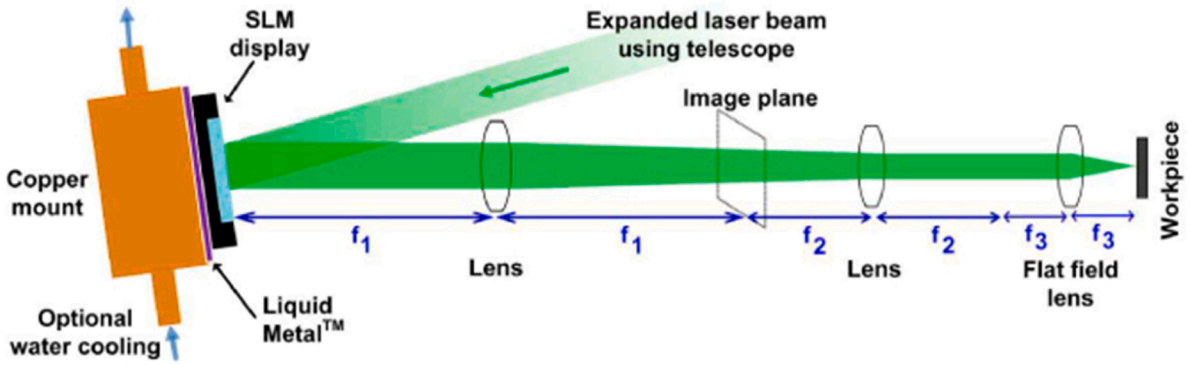

Fig. 13. Setup for laser machining using optical wavefront shaping using spatial light modulator. Reproduced with permission from [173].

modulated in real time by computer generated holograms. The patterns are generated at high throughput according to research by Kuang et al. Using this technique complex structures can be formed on the large surface area [172].

This shaping method can be used to laser process thin foil materials and is capable to produce high aspect ratio surface structures. One of the recent research by Sun et al. shows use of this technique to fabricate microporous arrays for oil–water separation application [174]. This process is also used to generate micro channels in the transparent polymer materials recently [175]. The optical wavefront shaping technique involves precise control of the spatial profile of the light wave, including both its amplitude and phase, to achieve the desired effect on the surface being processed. This technique can be used to generate a range of surface patterns and structures that can have different antifouling properties [128].

This is an approach to generate complex textures which are antifouling in nature effectively irrespective to materials, area and in cost effective way. However, this process is quite novel and under development and is in the initial phase of research and not being used commercially as large surface area processing is possible using this process.

4. Antifouling surfaces

There are various micro or nano topographic structures which increase fouling resistance properties and reduce the accumulation of foulants. These topographic structures can be replicated onto another material using the femtosecond micro or nano machining or structuring. This strategy is nontoxic and eco-friendly strategy to prevent fouling on surfaces.

4.1. Biomimetic surfaces

There are many nature inspired strategies in which the surfaces are designed by replicating the surface topology of that of some biological organism which can be termed as biomimetic surfaces, see Fig. 14. Other

strategies are controllable periodic structures which are repetitive structures which are fabricated using laser irradiation, laser induced graphene coating formation, and foam nano structuring.

Anti-biofouling approaches are found in the natural surfaces of different organisms. In the ambient environment plants such as rice leaves and insects employ these controls. In the marine environment plants, corals, and fish, crabs employ the physical and chemical controls of anti-fouling. Some of interesting surfaces are lotus leaves, taro leaves and shark skin which have property to prevent bacterial adhesion and cell attachment due to the presence of micro and nano super-hydrophobic structures and surface patterns which are present on them naturally These structures affects the wettability and adhesive properties of the surface which are function of the fouling resistance [176].

The self-cleaning behaviour is studied which is the effect of the micro and nano structures naturally present on the skin of the lotus leaf [177]. Furthermore, bacterial adhesion repletion was also studied on lotus leaf-inspired hierarchical, fluorinated polypropylene surfaces which were manufactured using reactive ion etching (RIE) treatments and it has been reported that best anti-biofouling results were obtained from fluorine reactive ion etched samples that created lotus leaf-like hierarchical structures consisting of microstructures and nanofibrils [178]. Furthermore, there is an ongoing research conducted on bioinspired self-cleaning and low drag micro/nanopatterned surfaces in mediums such as water, oil, and air flow based on the rice and butterfly wing which potentially prevents the colonization of microorganisms leading to biofouling [70]. Moreover, the research is focused on the anti-fouling properties of microstructure surfaces rice leaves and butterfly wings. Their study was focused on the anti-biofouling of E. coli microorganisms and have reported anti-inorganic fouling results from wash experiments using SiC simulated dirt particles [69]. Measurements and imaging were done using light microscopy and SEM. Contaminant removal was reported to be 95 % using the rice leaf pattern.

More interestingly, the gecko foot has some advanced surface properties such as antibacterial and self-cleaning [127]. The micro and nano structure of the skin exhibited ultralow adhesion with contaminating particles. The focus of the study was to investigate some of the associated properties/functions of this outer skin layer with a focus on solid and liquid contamination and it was found that gecko skin provides a unique topographical template for multifunctional man-made designs which may potentially aid in areas as diverse as self-cleaning surfaces [179].

The skin of the sharks is very intriguing three-dimensional rib patterns in their experimental study in oil flow channel optimization. The results show that shark skin reduced the drag significantly which also reduced the fouling which can be patterned onto different surfaces [181]. To support this a computational fluid dynamics study was conducted by researchers on a ship hull surface design. In their work, a comparison of surfaces one with biomimetic shark skin and another without showed that the hull with the biomimetic shark skin has better total drag coefficient with a reduction of about 9.5 % compared to the original hull. Drag reduction results from improved fouling resistance. The antifouling and friction reduction performance was also evaluated, and the results show that a remarkable improvement of 13 % was observed in fouling resistance and wettability as compared to the surface without the biomimetic shark skin. This was conducted using SEM analysis of the algae formation on the surface [182].

Moreover, in a recent study proposed biomimetic strategies and identified microstructures on the different marine shells such as Dosinia japonica, Gafrarium pectinatum and Mimachlamys nobilis which possess some antifouling properties. The researchers conducted anti-fouling trials on the replicated surface patterns on the polymer by measuring the chlorophyll-a content at different contact angles. The

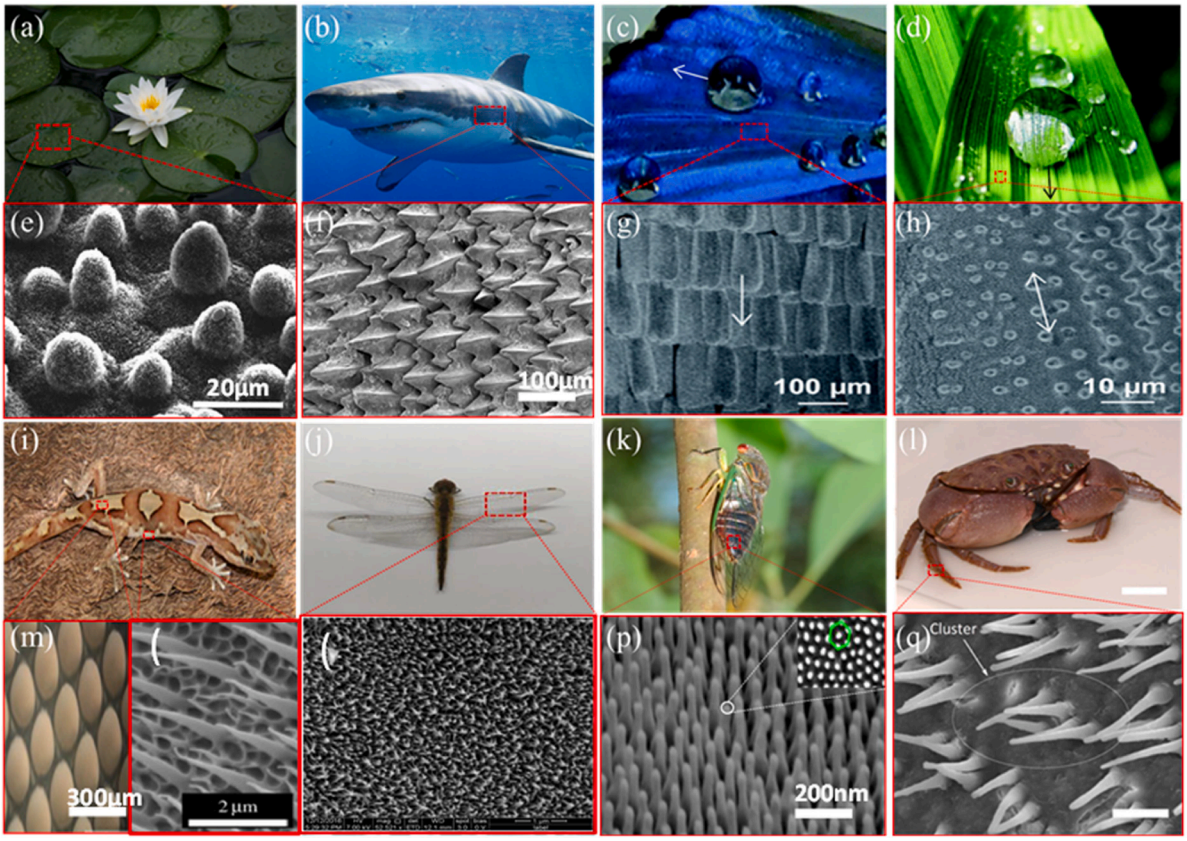

Fig. 14. Examples of bioinspired antifouling surfaces from different organisms such as (a) lotus leaf, (b) shark skin (c) butterfly wings, (d) rice leaf, (e- h) corresponding SEM images of the above examples, (i) geko (Lucasium steindachneri) (j) dragonfly of Pantala flavescens Fabricius (k) Psaltoda claripennis cicadae (l) marine decapod crab (M. hardwickii), (m-q) respective high magnification images of i, j, k and l. Reproduced with permission from references [180–184].

produced surfaces produced good fouling resistance. A lot of research has been conducted till now on biomimetic structure however it is still not complete as the replication of these structure on large surfaces is extremely costly. Studies need to be conducted for cost effective microstructures replication on large surfaces irrespective of their material which would increase the fouling resistance properties of the surfaces. The following section discusses some of important laser based micro and nano texturing techniques already being used in labs and industry [183].

4.2. Hierarchical micro periodic structures

Hierarchical textures, characterized by micron-scale patterns, can be engineered onto solid material surfaces to augment their hydrophobic properties, as illustrated in Fig. 15. These textures additionally incorporate sub-micron features that contribute to their improved resistance to fouling. Various artificial hierarchical textures, possessing periodic characteristics, exhibit the ability to deter the adhesion and aggregation of particles. Such textures can be readily manufactured on a variety of material surfaces. In recent study, conducted by Sun et al. by fabricating controlled periodic structures on AISI304 stainless steel substrate using picosecond laser system, and their anti-biofouling performance was examined by submersion of the substrate for five weeks in summertime [133]. A 50 % decrease of the average microbe attachment was obtained.

In another recent research by Tuo et al., superamphiphobic surfaces were developed on the 304 stainless steel and 6061 aluminium alloy surfaces using ultraviolet laser texturing and then coating with PTFE/FS-61 on the rough structures made by laser. The findings show that the surfaces exhibit excellent repellence to liquids such as water and oil. Moreover anti-fouling and drag reduction properties were also being reported [186]. These types of structures are useful when the fouling is at macro scale such as colloidal, scale, corrosion and ice fouling however micro-scale fouling is not much affected because of these structures such as biofouling which includes bacterial adhesion, protein adhesion or chemical fouling.

4.3. Nano scaled laser induced periodic surface structures

Laser induced periodic structures also known as LIPSS are the self-organized nano scaled structures produced by the laser irradiation of a material surface. LIPSS produces periodic ripple textures on the surface of the material with a spatial period (Λ). LIPSS are then broken down into two further categories based on the spatial period these are low spatial frequency LIPSS (LSFL) where the spatial period is roughly equal to the wavelength of the incident laser sources $\Lambda \sim \lambda$ and high spatial frequency LIPSS (HSFL) where $\Lambda \sim \lambda/3$ [187]. Due to the larger HAZ and less precise nature of short laser pulses only HSFL has being successfully synthesized using ultrashort pulse lasers [188]. The mechanism for the formation of LIPSS is still under consideration but the most widely accepted being Sipes theory which is based on the interference of the incident laser radiation with surface electromagnetic waves that are generated by scattering on the surface roughness [189]. The wavelength scale of the LIPSS texture makes it an ideal chose for the creation of ordered micro-nano structures which increase antifouling and hydrophobic behaviour [190].

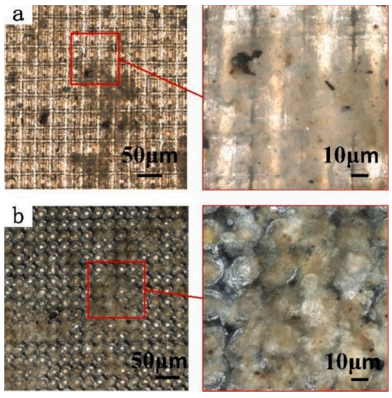

Fig. 15. Comparison of micro groove and pit patterns formed by controllable periodic structures using femtosecond laser (a) SHS with micro-groove pattern and (b) SHS with micro-pit pattern. Reproduced with permission from reference [185].

Laser etched surfaces produced surface properties that reduced bacterial adhesion and retention, see Fig. 16. Tri-modally dimensioned surface roughness, combined with a blunt conical macro-topography, and a close-packed fluoroalkyl monolayer, are shown to result in an optimised superhydrophobic surface that is highly resistant to bacterial adhesion, even under static inoculation conditions. It is anticipated that this approach could prove to be an important strategy for the development of antiadhesive surfaces in medical and industrial settings where biofouling is a significant problem [136].

The antifouling ability was tested for femtosecond laser produced periodic nanostructures by Epperlein et al., using the technique of purposefully colonizing E. coli and S. aureus bacteria [139]. Other work has also shown that femtosecond laser texturing can be applied to control bacterial colonization [191]. The results showed that the average fraction of surface area covered by bacteria on the laser-treated surface was 7 %, whereas the average fraction of surface area covered by the same bacteria on the polished sample was 25 %. This indicates a significant reduction of 18 % in bacterial adhesion on the laser-treated surface. The reduction in bacterial adhesion can be attributed to the fact that the features made by laser irradiation were slightly smaller than the size of the bacteria and denser, which hindered bacterial attachment. In addition to reduced bacterial adhesion, this study also reported a reduction in the tendency of S. aureus to form biofilms on the laser-treated surface. The results of this study demonstrate the potential of laser surface texturing as a technique for improving the antifouling ability of biomaterials. The nanoscale features produced by laser irradiation can effectively reduce bacterial adhesion and biofilm formation, which are major causes of implant failure and infections. Further studies are warranted to optimize the laser parameters and investigate the long-term efficacy of this technique.

4.4. Laser induced graphene

Graphene and graphene oxide are carbon-based nanomaterial with unique physical and electronic properties such as antibacterial, superhydrophobic, conduction [192]. Laser-induced graphene (LIG) has been shown to have antifouling properties [193,194]. LIG can resist bacterial attachment and reduce their viability when electrochemically activated [195]. It has been demonstrated that LIG coatings can resist bacteria accumulation and outperform control surfaces in reducing biofilm coverage [196]. LIG electrodes charged at low-voltage potentials have high antibacterial and antiviral performance [197]. The antibacterial and antiviral effects of LIG directly correlate to its capacitance, and the charged LIG electrodes maintain their antibacterial effect even after being stored [198]. Doped LIG devices, which can be fabricated using LIG, show biological antibacterial properties . These findings suggest that LIG has potential as an antifouling material for various applications, including environmental technology and water treatment . In recent work by Lin et al., direct laser writing was used using a CO_2 laser create a graphene oxide coating on a polymer surface which was found to be highly antifouling [199]. In research by Hoffman et al., the antibacterial activity of graphene-related materials, including graphite, graphite oxide, graphene oxide, and reduced graphene oxide, and their potential applications in nanoelectronics, conductive thin films, supercapacitors, nanosensors, and nanomedicine are discussed [200].

Also, according to recent research, graphene can be used for producing ultrafiltration membranes which have electrical conductivity

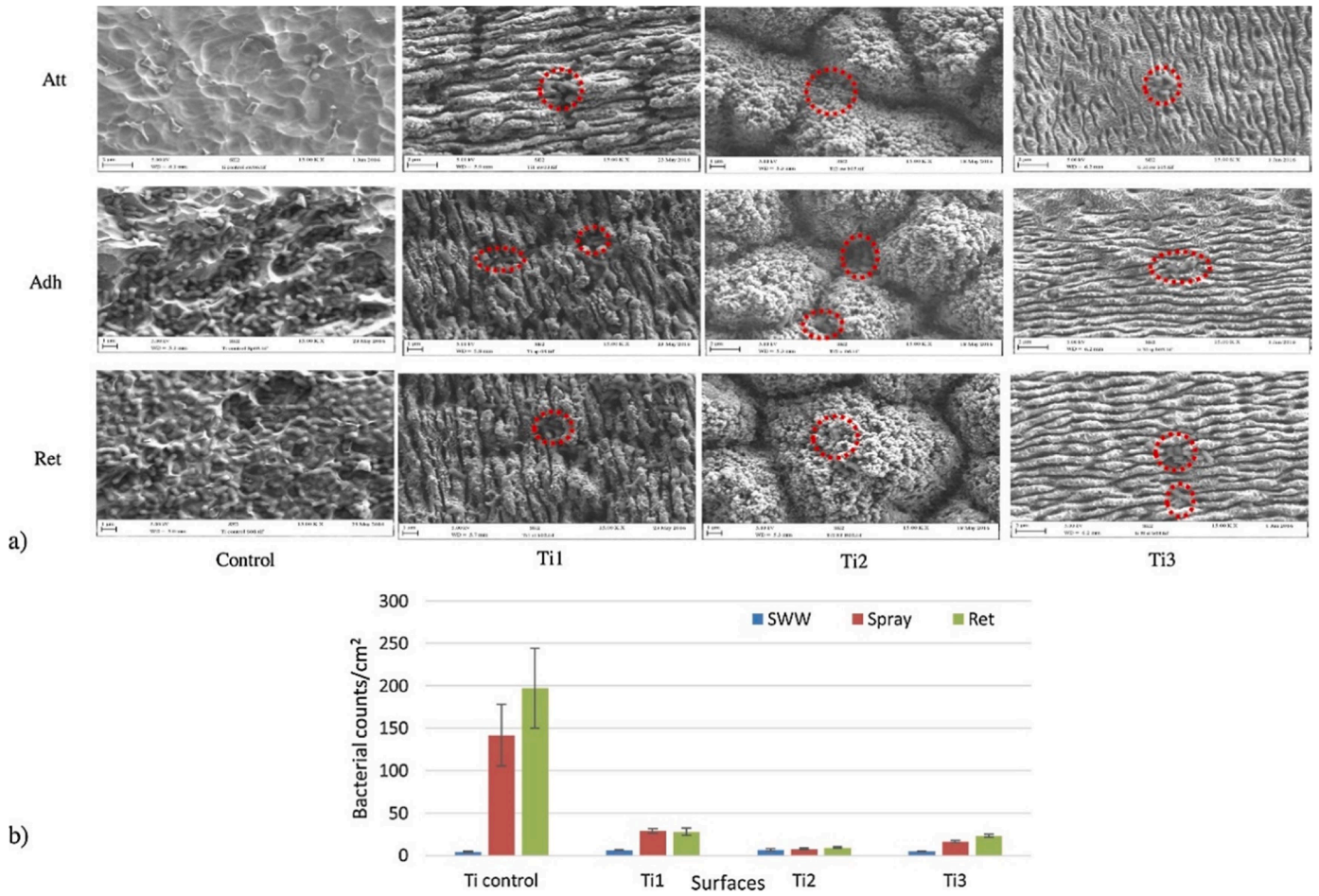

Fig. 16. (a) SEM image of laser induced periodic surface structures to enhance antifouling properties and (b) numbers of bacteria retained on the surfaces following attachment (SWW), adhesion (Spray) and retention assays (Ret) Reproduced with permission from reference [136].

and antifouling properties [142]. The results show that because of increasing the amount of crosslinked graphene oxide on the laser induced graphene (LIG) surface resulted in increased removal of bovine serum albumin (BSA) up to 69 %, and bacterial rejection was improved from 20 % to 99.9 %. Hence the composite membranes showed significantly less biofilm growth compared to a typical polymer ultrafiltration membrane. These graphene oxides are used in the water filtration and desalination application [201]. LIG also has excellent mechanical properties and chemical stability, making it a promising material for membrane applications. However, further research is needed to fully explore the potential of LIG as an antifouling material for membrane applications and to optimize the fabrication and performance of LIG-based membranes.

5. Conclusion and future perspectives

As the demand for sustainable and efficient antifouling surfaces continues to grow, laser texturing is expected to play a crucial role in the development of new and innovative solutions. With the increasing interest in this field, effective and long-lasting anti-fouling surface fabrication can bring significant technical advantages and economic benefits. This review paper provides a comprehensive overview of the latest developments in anti-fouling surface science and engineering. The paper covers a range of surface fouling methods, physical surface nano and micro-scale texture production methods, and biomimetic antifouling surfaces. However even with the development of so many physical, chemical and combination techniques there are many challenges for fabricating an effective antifouling surface. Ultrafast laser surface texturing has emerged as a promising technique for producing antifouling surfaces due to its ability to accurately, precisely and repeatably alter the physical and chemical properties of surfaces. However, there are several remaining challenges.

One major challenge is the need for antifouling surfaces to be durable and long-lasting. Many antifouling textures and materials degrade over time, reducing their effectiveness at preventing fouling. The harsh conditions in which many antifouling surfaces are used, such as exposure to seawater or harsh chemicals, can cause degradation of the textures, making it less effective over time. Developing materials that can withstand these harsh conditions and maintain their antifouling properties is a significant challenge [202].

Another challenge is the need for antifouling surfaces to be non-toxic and environmentally friendly. Many traditional antifouling coatings contain toxic chemicals, such as copper and tributyltin, that can have harmful effects on marine life and the environment. Developing texturing strategies and materials that are effective at preventing fouling but which do not contain harmful chemicals is a significant challenge [203,204].

Moreover, there is a lack of understanding of the mechanisms involved in laser-induced textures which are inherently antifouling. While it is known that laser treatment can alter surface properties such as roughness, hydrophobicity, and surface energy, the specific mechanisms by which these alterations prevent fouling organisms from adhering to surfaces are fully understood. This makes it difficult to optimize laser parameters to produce the desired antifouling properties.

Another challenge is the variability in laser treatment outcomes. Laser treatment can produce highly variable results depending on

factors such as laser power, pulse duration, and other process parameters. This variability can make it difficult to reproduce desired antifouling properties across different surfaces and experimental conditions. Additionally, the surface chemistry of the substrate can also play a significant role in the effectiveness of laser treatment for antifouling, adding another layer of complexity.

Furthermore, the cost of producing antifouling surfaces using lasers can be high. Laser equipment and maintenance can be expensive, and the process can be time-consuming for very large surfaces. Although with more recent high-speed optics the process rates for large surface areas have improved.

Finally, there is a need for standardized testing methods for evaluating the efficacy of laser-treated antifouling surfaces. It is difficult to compare results across studies and to assess the effectiveness of different laser treatments for antifouling [205]. While various techniques such as biofilm assays and microbial adhesion assays exist, there is a need to increase the use of standards for quantifying fouling in a systematic manner.

To fill these knowledge and implementation gaps further investigation of the effects of the laser process parameters on surface morphology and surface fouling, the development of standardized test methods for antifouling surface characterization, and the development of cost-effective ultrashort laser setups are required.

Declaration of Competing Interest

The authors declare that they have no known competing financial interests or personal relationships that could have appeared to influence the work reported in this paper.

Data availability

Data will be made available on request.

Acknowledgments

This publication has emanated from research supported by Science Foundation Ireland (SFI) under Grant Numbers 16/RC/3872 and 18/EPSRC-CDT/3584; and is co-funded under the European Regional Development Fund and by I-Form industry partners, from the European Union's Horizon 2020 Research and Innovation Programme under grant agreement No. 862100.

References

[1] C. Bressy, M. Lejars, Marine fouling : an overview marine fouling, J. Ocean Technol. 9 (2014) 19–28.
[2] N.D. Bureau of Ships, Marine fouling and its prevention, United States Naval Institute, 1952. 10.1575/1912/191.
[3] M.D. Richmond, R. Seed, A review of marine macrofouling communities with special reference to animal fouling, Biofouling 3 (1991) 151–168, https://doi.org/10.1080/08927019109378169.
[4] S. Cao, J.D. Wang, H.S. Chen, D.R. Chen, Progress of marine biofouling and antifouling technologies, Chinese Sci. Bull. 56 (2011) 598–612, https://doi.org/10.1007/s11434-010-4158-4.
[5] A. Volpe, C. Gaudiuso, A. Ancona, Laser fabrication of anti-icing surfaces: a review, Material 13 (2020) 5692, https://doi.org/10.3390/MA13245692, 2020, Vol. 13, Page 5692.
[6] E.Grant Jones, W.J. Balster, Surface fouling in aviation fuel: short- vs long-term isothermal tests, Energy Fuels 9 (1995) 610–615, https://doi.org/10.1021/EF00052A006.
[7] U. Igie, M. Goiricelaya, D. Nalianda, O. Minervino, Aero engine compressor fouling effects for short-and long-haul missions, Proc. Inst. Mech. Eng. Part G J. Aerosp. Eng. 230 (2016) 1312–1324, https://doi.org/10.1177/0954410015607897.
[8] X. Huang, N. Tepylo, V. Pommier-Budinger, M. Budinger, E. Bonaccurso, P. Villedieu, L. Bennani, A survey of icephobic coatings and their potential use in a hybrid coating/active ice protection system for aerospace applications, Prog. Aerosp. Sci. 105 (2019) 74–97, https://doi.org/10.1016/J.PAEROSCI.2019.01.002.
[9] N. Dalili, A. Edrisy, R. Carriveau, A review of surface engineering issues critical to wind turbine performance, Renew. Sustain. Energy Rev. 13 (2009) 428–438, https://doi.org/10.1016/j.rser.2007.11.009.
[10] J.L. Laforte, M.A. Allaire, J. Laflamme, State-of-the-art on power line de-icing, Atmos. Res. 46 (1998) 143–158, https://doi.org/10.1016/S0169-8095(97)00057-4.
[11] R.M. Fillion, A.R. Riahi, A. Edrisy, A review of icing prevention in photovoltaic devices by surface engineering, Renew. Sustain. Energy Rev. 32 (2014) 797–809, https://doi.org/10.1016/J.RSER.2014.01.015.
[12] D. Wilhelmsson, T. Malm, Fouling assemblages on offshore wind power plants and adjacent substrata, Estuar. Coast. Shelf Sci. 79 (2008) 459–466, https://doi.org/10.1016/J.ECSS.2008.04.020.
[13] V.B. Damodaran, S.N. Murthy, Bio-inspired strategies for designing antifouling biomaterials, Biomater. Res. 20 (2016) 1–11, https://doi.org/10.1186/s40824-016-0064-4.
[14] J.L. Harding, M.M. Reynolds, Combating medical device fouling, Trends Biotechnol. 32 (2014) 140–146, https://doi.org/10.1016/j.tibtech.2013.12.004.
[15] I. Francolini, C. Vuotto, A. Piozzi, G. Donelli, Antifouling and antimicrobial biomaterials: an overview, APMIS 125 (2017) 392–417, https://doi.org/10.1111/apm.12675.
[16] E.J. Falde, S.T. Yohe, Y.L. Colson, M.W. Grinstaff, Superhydrophobic materials for biomedical applications, Biomaterials 104 (2016) 87–103, https://doi.org/10.1016/J.BIOMATERIALS.2016.06.050.
[17] M. Zupančič, D. Novak, J. Diaci, I. Golobič, An evaluation of industrial ultrafiltration systems for surface water using fouling indices as a performance indicator, Desalination 344 (2014) 321–328, https://doi.org/10.1016/J.DESAL.2014.04.002.
[18] D.I. Wilson, Fouling during food processing – Progress in tackling this inconvenient truth, Curr. Opin. Food Sci. 23 (2018) 105–112, https://doi.org/10.1016/j.cofs.2018.10.002.
[19] F.G.F. Qin, A.B. Russell, X.D. Chen, L. Robertson, Ice fouling on a subcooled metal surface examined by thermo-response and electrical conductivity, J. Food Eng. 59 (2003) 421–429, https://doi.org/10.1016/S0260-8774(03)00002-5.
[20] J.A. Barish, J.M. Goddard, Anti-fouling surface modified stainless steel for food processing, Food Bioprod. Process. 91 (2013) 352–361, https://doi.org/10.1016/j.fbp.2013.01.003.
[21] T. Mérian, J.M. Goddard, Advances in nonfouling materials: perspectives for the food industry, J. Agric. Food Chem. 60 (2012) 2943–2957, https://doi.org/10.1021/JF204741P/ASSET/IMAGES/LARGE/JF-2011-04741P_0003.JPEG.
[22] H. Bleile, S.D. Rodgers, Marine Coatings, in: Proceedings of the Encyclopedia of Materials: Science and Technology, 2001, pp. 5174–5185, https://doi.org/10.1016/b0-08-043152-6/00899-8.
[23] D.M. Yebra, S. Kiil, K. Dam-Johansen, Antifouling technology-past, present and future steps towards efficient and environmentally friendly antifouling coatings, Prog. Org. Coat. 50 (2004) 75–104, https://doi.org/10.1016/j.porgcoat.2003.06.001.
[24] D. Strickland, G. Mourou, Compression of amplified chirped optical pulses, Opt. Commun. 55 (1985) 447–449, https://doi.org/10.1016/0030-4018(85)90151-8.
[25] S. Kawabata, S. Bai, K. Obata, G. Miyaji, K. Sugioka, Two-dimensional laser-induced periodic surface structures formed on crystalline silicon by GHz burst mode femtosecond laser pulses, Int. J. Extrem. Manuf. 5 (2023), https://doi.org/10.1088/2631-7990/acb133.
[26] K. Sugioka, Y. Cheng, Ultrafast lasers-reliable tools for advanced materials processing, Light Sci. Appl. 3 (2014), https://doi.org/10.1038/lsa.2014.30.
[27] J. Yong, F. Chen, Q. Yang, Y. Fang, J. Huo, J. Zhang, X. Hou, Nepenthes inspired design of self-repairing omniphobic slippery liquid infused porous surface (SLIPS) by femtosecond laser direct writing, Adv. Mater. Interfaces 4 (2017) 1–7, https://doi.org/10.1002/admi.201700552.
[28] Y. Yuan, H. Xiang, G. Liu, L. Wang, H. Liu, R. Liao, Self-repairing performance of slippery liquid infused porous surfaces for durable anti-icing, Adv. Mater. Interfaces 9 (2022) 1–10, https://doi.org/10.1002/admi.202101968.
[29] H.H. Tran, D. Lee, D. Riassetto, Wetting ridges on slippery liquid-infused porous surfaces, Rep. Prog. Phys. 86 (2023), https://doi.org/10.1088/1361-6633/acc87a.
[30] C. Wang, Z. Guo, A comparison between superhydrophobic surfaces (SHS) and slippery liquid-infused porous surfaces (SLIPS) in application, Nanoscale 12 (2020) 22398–22424, https://doi.org/10.1039/d0nr06009g.
[31] L. Li, Y. Bai, L. Li, S. Wang, T. Zhang, A superhydrophobic smart coating for flexible and wearable sensing electronics, Adv. Mater. 29 (2017) 1–8, https://doi.org/10.1002/adma.201702517.
[32] C. Yao, S. Xu, X. Jiang, J. Chen, X. Yuan, A simple way to achieve self-cleaning surfaces with unique antifouling property, J. Chem. 2020 (2020), https://doi.org/10.1155/2020/9072432.
[33] A.K. Halvey, B. Macdonald, A. Dhyani, A. Tuteja, Design of surfaces for controlling hard and soft fouling, Philos. Trans. R. Soc. A Math. Phys. Eng. Sci. 377 (2019), https://doi.org/10.1098/rsta.2018.0266.
[34] P.H. Lin, B.R. Li, Antifouling strategies in advanced electrochemical sensors and biosensors, Analyst 145 (2020) 1110–1120, https://doi.org/10.1039/C9AN02017A.
[35] M.T. Brunelle, Colloidal fouling of reverse osmosis membranes, Desalination 32 (1980) 127–135, https://doi.org/10.1016/S0011-9164(00)86013-0.
[36] M. Bohnet, Fouling of heat transfer surfaces, Chem. Eng. Technol. 10 (1987) 113–125, https://doi.org/10.1002/CEAT.270100115.
[37] S.N. Kazi, Fouling and fouling mitigation on heat exchanger surfaces, Heat Exch. Basics Des. Appl. (2012), https://doi.org/10.5772/32990.

[38] A.P. Watkinson, Chemical reaction fouling of organic fluids, Chem. Eng. Technol. 15 (1992) 82–90, https://doi.org/10.1002/ceat.270150203.
[39] A.P. Watkinson, D.I. Wilson, Chemical reaction fouling: a review, Exp. Therm. Fluid Sci. 14 (1997) 361–374, https://doi.org/10.1016/S0894-1777(96)00138-0.
[40] G.A. Jacobson, Corrosion basics - NACE, (2020). https://www.nace.org/resources/general-resources/corrosion-basics (accessed May 19, 2021).
[41] E.F.C. Somerscales, Fundamentals of corrosion fouling, Exp. Therm. Fluid Sci. 14 (1997) 335–355, https://doi.org/10.1016/S0894-1777(96)00136-7.
[42] Y. Li, C. Ning, Latest research progress of marine microbiological corrosion and bio-fouling, and new approaches of marine anti-corrosion and anti-fouling, Bioact. Mater. 4 (2019) 189–195, https://doi.org/10.1016/j.bioactmat.2019.04.003.
[43] S. Permeh, K. Lau, M. Duncan, Degradation of coatings for steel in environments susceptible to corrosion associated with fouling, Struct. Infrastruct. Eng. 16 (2020) 1186–1200, https://doi.org/10.1080/15732479.2019.1694543.
[44] E.F.C. Somerscales, M. Kassemi, Fouling due to corrosion products formed on a heat transfer surface, J. Heat Transf. 109 (1987) 267–271, https://doi.org/10.1115/1.3248061.
[45] J.W. Costerton, Marine and Industrial Biofouling, Springer-Verlag, Berlin Heidelberg, 2009, https://doi.org/10.1007/978-3-540-69796-1.
[46] C.M. Magin, S.P. Cooper, A.B. Brennan, Non-toxic antifouling strategies, Mater. Today 13 (2010) 36–44, https://doi.org/10.1016/S1369-7021(10)70058-4.
[47] W. Guo, H.H. Ngo, J. Li, A mini-review on membrane fouling, Bioresour. Technol. 122 (2012) 27–34, https://doi.org/10.1016/j.biortech.2012.04.089.
[48] G. Amy, Fundamental understanding of organic matter fouling of membranes, Desalination 231 (2008) 44–51, https://doi.org/10.1016/J.DESAL.2007.11.037.
[49] M.P. Schultz, J.A. Bendick, E.R. Holm, W.M. Hertel, Economic impact of biofouling on a naval surface ship, Biofouling 27 (2011) 87–98, https://doi.org/10.1080/08927014.2010.542809.
[50] A. Farkas, N. Degiuli, I. Martić, The impact of biofouling on the propeller performance, Ocean Eng. 219 (2021), 108376, https://doi.org/10.1016/j.oceaneng.2020.108376.
[51] K. Rykaczewski, S. Anand, S.B. Subramanyam, K.K. Varanasi, Mechanism of frost formation on lubricant-impregnated surfaces, Langmuir 29 (2013) 5230–5238, https://doi.org/10.1021/la400801s.
[52] S.K. Thomas, R.P. Cassoni, C.D. MacArthur, Aircraft anti-icing and de-icing techniques and modeling, J. Aircr. 33 (1996) 841–854, https://doi.org/10.2514/3.47027.
[53] R. Carriveau, A. Edrisy, P. Cadieux, R. Mailloux, Ice adhesion issues in renewable energy infrastructure, J. Adhes. Sci. Technol. 26 (2012) 447–461, https://doi.org/10.1163/016942411X574592.
[54] J.A. Callow, M.E. Callow, Trends in the development of environmentally friendly fouling-resistant marine coatings, Nat. Commun. 2 (2011) 1–10, https://doi.org/10.1038/ncomms1251, 2011 21.
[55] A.J. Scardino, D. Hudleston, Z. Peng, N.A. Paul, R. De Nys, Biomimetic characterisation of key surface parameters for the development of fouling resistant materials, Biofouling 25 (2009) 83–93, https://doi.org/10.1080/08927010802538480.
[56] B.A.B D Cassie, S. Baxter, Wettability of porous surfaces, Trans. Faraday Soc. 40 (1944) 546–551.
[57] J. Jeevahan, M. Chandrasekaran, G. Britto Joseph, R.B. Durairaj, G. Mageshwaran, Superhydrophobic surfaces: a review on fundamentals, applications, and challenges, J. Coatings Technol. Res. 15 (2018) 231–250, https://doi.org/10.1007/s11998-017-0011-x.
[58] R. Jagdheesh, M. Diaz, J.L. Ocaña, Bio inspired self-cleaning ultrahydrophobic aluminium surface by laser processing, RSC Adv. 6 (2016) 72933–72941, https://doi.org/10.1039/c6ra12236a.
[59] A. Khaskhoussi, L. Calabrese, E. Proverbio, Effect of the Cassie Baxter-Wenzel behaviour transitions on the corrosion performances of AA6082 superhydrophobic surfaces, Metall. Ital. 113 (2021) 15–21.
[60] J. Long, P. Fan, D. Gong, D. Jiang, H. Zhang, L. Li, M. Zhong, Superhydrophobic surfaces fabricated by femtosecond laser with tunable water adhesion: from lotus leaf to rose petal, ACS Appl. Mater. Interfaces 7 (2015) 9858–9865, https://doi.org/10.1021/ACSAMI.5B01870/SUPPL_FILE/AM5B01870_SI_001.AVI.
[61] D. Behnoudfar, M.I. Dragila, D. Meisenheimer, D. Wildenschild, Contact angle hysteresis: a new paradigm? Adv. Water Resour. 161 (2022), 104138 https://doi.org/10.1016/j.advwatres.2022.104138.
[62] A. Volpe, C. Gaudiuso, A. Ancona, Laser fabrication of anti-icing surfaces: a review, Materials 13 (2020) 1–24, https://doi.org/10.3390/ma13245692 (Basel).
[63] G. Perumal, A. Chakrabarti, H.S. Grewal, S. Pati, S. Singh, H.S. Arora, Enhanced antibacterial properties and the cellular response of stainless steel through friction stir processing, 10.1080/08927014.2019.1584794. 35 (2019) 187–203. 10.1080/08927014.2019.1584794.
[64] D. Wei, A. Ivaska, Electrochemical biosensors based on polyaniline, Chem. Analityczna 51 (2006) 839–852.
[65] Q. Liu, X. Zhou, H. Wu, L. Wu, B. Zheng, A polydopamine patterned perfluoropolymer-based substrate for protein microarray applications, Sens. Actuators B Chem. 287 (2019) 306–311, https://doi.org/10.1016/j.snb.2019.02.064.
[66] K. Yajima, K. Adachi, Y. Tsukahara, J. Taniguchi, Fabrication of antireflection structure with antifouling-effect surface by ultraviolet nanoimprint lithography, Microelectron. Eng. 110 (2013) 188–191, https://doi.org/10.1016/j.mee.2013.03.104.
[67] O.P.A. Trautmann, F. Heuck, C. Mueller, P. Ruther, Replication of microneedle arrays using vacuum casting and hot embossing, in: Proceedings of the 13 International Conference Solid State Sensors, Actuators Microsystems, IEEE Explore, Seoul, Korea, 2005, pp. 1420–1423, https://doi.org/10.1109/SENSOR.2005.1497348.
[68] A. Al-Shimmery, S. Mazinani, J. Ji, Y.M.J. Chew, D. Mattia, 3D printed composite membranes with enhanced anti-fouling behaviour, J. Memb. Sci. 574 (2019) 76–85, https://doi.org/10.1016/j.memsci.2018.12.058.
[69] G.D. Bixler, A. Theiss, B. Bhushan, S.C. Lee, Anti-fouling properties of microstructured surfaces bio-inspired by rice leaves and butterfly wings, J. Colloid Interface Sci. 419 (2014) 114–133, https://doi.org/10.1016/j.jcis.2013.12.019.
[70] G.D. Bixler, B. Bhushan, Rice- and butterfly-wing effect inspired self-cleaning and low drag micro/nanopatterned surfaces in water, oil, and air flow, Nanoscale 6 (2014) 76–96, https://doi.org/10.1039/c3nr04755e.
[71] T. Li, M. Paliy, X. Wang, B. Kobe, W.M. Lau, J. Yang, Facile one-step photolithographic method for engineering hierarchically nano/microstructured transparent superamphiphobic surfaces, ACS Appl. Mater. Interfaces 7 (2015) 10988–10992, https://doi.org/10.1021/acsami.5b01926.
[72] C. Credi, C. De Marco, E. Molena, M.M. Nava, M.T. Raimondi, M. Levi, S. Turri, Direct photo-patterning of hyaluronic acid baits onto a fouling-release perfluoropolyether surface for selective cancer cell capture and immobilization, Mater. Sci. Eng. C 62 (2016) 414–422, https://doi.org/10.1016/j.msec.2015.12.063.
[73] M. Parracino, P. Pellacani, P. Colpo, G. Ceccone, A. Valsesia, F. Rossi, M. Manso Silvan, Biofouling properties of nitroxide-modified amorphous carbon surfaces, ACS Biomater. Sci. Eng. 2 (2016) 1976–1982, https://doi.org/10.1021/acsbiomaterials.6b00381.
[74] P. Sae-Ung, K.W. Kolewe, Y. Bai, E.W. Rice, J.D. Schiffman, T. Emrick, V. P. Hoven, Antifouling stripes prepared from clickable zwitterionic copolymers, Langmuir 33 (2017) 7028–7035, https://doi.org/10.1021/acs.langmuir.7b01431.
[75] K. Solin, H. Orelma, M. Borghei, M. Vuoriluoto, R. Koivunen, O.J. Rojas, Two-dimensional antifouling fluidic channels on nanopapers for biosensing, Biomacromolecules 20 (2019) 1036–1044, https://doi.org/10.1021/acs.biomac.8b01656.
[76] J. Taniguchi, E. Yamauchi, Y. Nemoto, Fabrication of antireflection structures on glassy carbon surfaces using electron beam lithography and oxygen dry etching, J. Phys. Conf. Ser. 106 (2008) 12011, https://doi.org/10.1088/1742-6596/106/1/012011.
[77] N.W. Parker, A.D. Brodie, J.H. McCoy, High-throughput NGL electron-beam direct-write lithography system</title>, in: Proceedings of the Emerging Lithographic Technologies IV, SPIE, 2000, pp. 713–720, https://doi.org/10.1117/12.390042.
[78] M.V. Graham, A.P. Mosier, T.R. Kiehl, A.E. Kaloyeros, N.C. Cady, Development of antifouling surfaces to reduce bacterial attachment, Soft Matter 9 (2013) 6235–6244, https://doi.org/10.1039/c3sm50584g.
[79] F. Watt, A.A. Bettiol, J.A. Van Kan, E.J. Teo, M.B.H. Breese, Ion beam lithography and nanofabrication: a review, Int. J. Nanosci. 4 (2005) 269–286, https://doi.org/10.1142/S0219581X05003139.
[80] G. Dos Reis, F. Fenili, A. Gianfelice, G. Bongiorno, D. Marchesi, P.E. Scopelliti, A. Borgonovo, A. Podestà, M. Indrieri, E. Ranucci, P. Ferruti, C. Lenardi, P. Milani, Direct microfabrication of topographical and chemical cues for the guided growth of neural cell networks on polyamidoamine hydrogels, Macromol. Biosci. 10 (2010) 842–852, https://doi.org/10.1002/mabi.200900410.
[81] X. Wu, F. Teng, M. Libera, Functional changes during electron-beam lithography of biotinylated poly(ethylene glycol) thin films, ACS Macro Lett. 8 (2019) 1252–1256, https://doi.org/10.1021/acsmacrolett.9b00585.
[82] J.E.E. Baglin, Ion beam nanoscale fabrication and lithography - A review. Appl. Surf. Sci., 2012, pp. 4103–4111, https://doi.org/10.1016/j.apsusc.2011.11.074. Elsevier B.V.
[83] W. Zheng, W. Zhang, X. Jiang, Precise control of cell adhesion by combination of surface chemistry and soft lithography, Adv. Healthc. Mater. 2 (2013) 95–108, https://doi.org/10.1002/adhm.201200104.
[84] G. Tullii, S. Donini, C. Bossio, F. Lodola, M. Pasini, E. Parisini, F. Galeotti, M. R. Antognazza, Micro- and nanopatterned silk substrates for antifouling applications, ACS Appl. Mater. Interfaces 12 (2020) 5437–5446, https://doi.org/10.1021/acsami.9b18187.
[85] M.A. Rose, J.J. Bowen, S.A. Morin, Emergent soft lithographic tools for the fabrication of functional polymeric microstructures, ChemPhysChem 20 (2019) 909–925, https://doi.org/10.1002/cphc.201801140.
[86] M. Xie, W. Luo, S.R. Gray, Surface pattern by nanoimprint for membrane fouling mitigation: design, performance and mechanisms, Water Res. 124 (2017) 238–243, https://doi.org/10.1016/j.watres.2017.07.057.
[87] Y. Ding, S. Maruf, M. Aghajani, A.R. Greenberg, Surface patterning of polymeric membranes and its effect on antifouling characteristics, Sep. Sci. Technol. 52 (2017) 240–257, https://doi.org/10.1080/01496395.2016.1201115.
[88] L.S. Wang, A. Gupta, B. Duncan, R. Ramanathan, M. Yazdani, V.M. Rotello, Biocidal and antifouling chlorinated protein films, ACS Biomater. Sci. Eng. 2 (2016) 1862–1866, https://doi.org/10.1021/acsbiomaterials.6b00464.
[89] F. Dundar Arisoy, K.W. Kolewe, B. Homyak, I.S. Kurtz, J.D. Schiffman, J. J. Watkins, Bioinspired photocatalytic shark-skin surfaces with antibacterial and antifouling activity via nanoimprint lithography, ACS Appl. Mater. Interfaces 10 (2018) 20055–20063, https://doi.org/10.1021/acsami.8b05066.
[90] G. Zhang, J. Zhang, G. Xie, Z. Liu, H. Shao, Cicada wings: a stamp from nature for nanoimprint lithography, Small 2 (2006) 1440–1443, https://doi.org/10.1002/smll.200600255.

[91] Y. Wang, M. Zhang, Y. Lai, L. Chi, Advanced colloidal lithography: from patterning to applications, Nano Today 22 (2018) 36–61, https://doi.org/10.1016/j.nantod.2018.08.010.
[92] W. Liu, X. Liu, J. Fangteng, S. Wang, L. Fang, H. Shen, S. Xiang, H. Sun, B. Yang, Bioinspired polyethylene terephthalate nanocone arrays with underwater superoleophobicity and anti-bioadhesion properties, Nanoscale 6 (2014) 13845–13853, https://doi.org/10.1039/c4nr04471a.
[93] M. Sayin, R. Dahint, Formation of charge-nanopatterned templates with flexible geometry via layer by layer deposition of polyelectrolytes for directed self-assembly of gold nanoparticles, Nanotechnology 28 (2017), 135303, https://doi.org/10.1088/1361-6528/aa5ec3.
[94] P. Kothary, X. Dou, Y. Fang, Z. Gu, S.Y. Leo, P. Jiang, Superhydrophobic hierarchical arrays fabricated by a scalable colloidal lithography approach, J. Colloid Interface Sci. 487 (2017) 484–492, https://doi.org/10.1016/j.jcis.2016.10.081.
[95] Y. Zhan, J. Zhao, W. Liu, B. Yang, J. Wei, Y. Yu, Biomimetic submicroarrayed cross-linked liquid crystal polymer films with different wettability via colloidal lithography, ACS Appl. Mater. Interfaces 7 (2015) 25522–25528, https://doi.org/10.1021/acsami.5b09013.
[96] Y.W.M.J.D.T.S. Zhang, Micro-moulded magnetic artificial cilia for anti-fouling surfaces — Eindhoven University of Technology research portal, in: Proceedings of the International MicroNanoConference (IMNC 2016) - Beurs van Berlage Amsterdam, Amsterdam, Netherlands, 2016. https://research.tue.nl/en/publications/micro-moulded-magnetic-artificial-cilia-for-anti-fouling-surfaces (accessed May 24, 2021).
[97] C. Delaney, N. Geoghegan, H. Ibrahim, M. O'Loughlin, B.J. Rodriguez, L. Florea, S.M. Kelleher, Direct laser writing to generate molds for polymer nanopillar replication, ACS Appl. Polym. Mater. 2 (2020) 3632–3641, https://doi.org/10.1021/acsapm.0c00626.
[98] M. Denoual, Y. Macé, B. Le Pioufle, P. Mognol, D. Castel, M. Denoual, B. Le Pioufle, P. Mognol, X. Gidrol, Vacuum casting to manufacture a plastic biochip for highly parallel cell transfection, Meas. Sci. Technol. 17 (2006), https://doi.org/10.1088/0957-0233/17/12/S03ï.
[99] T.W. Kim, Assessment of hydro/oleophobicity for shark skin replica with riblets, J. Nanosci. Nanotechnol. 14 (2014) 7562–7568, https://doi.org/10.1166/jnn.2014.9570.
[100] D.Y. Zhao, Z.P. Huang, M.J. Wang, T. Wang, Y. Jin, Vacuum casting replication of micro-riblets on shark skin for drag-reducing applications, J. Mater. Process. Technol. 212 (2012) 198–202, https://doi.org/10.1016/j.jmatprotec.2011.09.002.
[101] B. Kim, S.B. Seo, K. Bae, D.Y. Kim, C.H. Baek, H.M. Kim, Stable superhydrophobic si surface produced by using reactive ion etching process combined with hydrophobic coatings, Surf. Coat. Technol. 232 (2013) 928–935, https://doi.org/10.1016/j.surfcoat.2013.07.002.
[102] B. Kim, H. Kim, J. Kim, C.S. Cho, J. Lee, Superhydrophobic polytetrafluoroethylene surface obtained using reactive ion etching and duplication with polydimethylsiloxane mould, Micro Nano Lett. (2013) 691–695, https://doi.org/10.1049/mnl.2013.0266. The Institution of Engineering and Technology.
[103] M. Munther, T. Palma, I.A. Angeron, S. Salari, H. Ghassemi, M. Vasefi, A. Beheshti, K. Davami, Microfabricated biomimetic placoid scale-inspired surfaces for antifouling applications, Appl. Surf. Sci. 453 (2018) 166–172, https://doi.org/10.1016/j.apsusc.2018.05.030.
[104] D. Ebert, B. Bhushan, Transparent, superhydrophobic, and wear-resistant surfaces using deep reactive ion etching on PDMS substrates, J. Colloid Interface Sci. 481 (2016) 82–90, https://doi.org/10.1016/j.jcis.2016.07.035.
[105] M. Ganjian, K. Modaresifar, H. Zhang, P.L. Hagedoorn, L.E. Fratila-Apachitei, A. A. Zadpoor, Reactive ion etching for fabrication of biofunctional titanium nanostructures, Sci. Rep. 9 (2019) 1–20, https://doi.org/10.1038/s41598-019-55093-y.
[106] S. Ma, Q. Ye, X. Pei, D. Wang, F. Zhou, Antifouling on Gecko's feet inspired fibrillar surfaces: evolving from land to marine and from liquid repellency to algae resistance, Adv. Mater. Interfaces 2 (2015), 1500257, https://doi.org/10.1002/admi.201500257.
[107] N. Kodihalli Shivaprakash, J. Zhang, T. Nahum, C. Barry, Q. Truong, J. Mead, Roll-to-roll hot embossing of high aspect ratio micro pillars for superhydrophobic applications, Int. Polym. Process. 34 (2019) 502–512, https://doi.org/10.3139/217.3815.
[108] J. Li, W. Yu, D. Zheng, X. Zhao, C.H. Choi, G. Sun, Hot embossing for whole Teflon superhydrophobic surfaces, Coatings 8 (2018) 227, https://doi.org/10.3390/coatings8070227.
[109] C. Yan, P. Jiang, X. Jia, X. Wang, 3D printing of bioinspired textured surfaces with superamphiphobicity, Nanoscale 12 (2020) 2924–2938, https://doi.org/10.1039/c9nr09620e.
[110] Z. Lyu, T.C.A. Ng, T. Tran-Duc, G.J.H. Lim, Q. Gu, L. Zhang, Z. Zhang, J. Ding, N. Phan-Thien, J. Wang, H.Y. Ng, 3D-printed surface-patterned ceramic membrane with enhanced performance in crossflow filtration, J. Memb. Sci. 606 (2020), 118138, https://doi.org/10.1016/j.memsci.2020.118138.
[111] R. Piola, M. Leary, R. Santander, J. Shimeta, Antifouling performance of copper-containing fused filament fabrication (FFF) 3-D printing polymer filaments for marine applications, Biofouling 37 (2021) 206–221, https://doi.org/10.1080/08927014.2021.1892085.
[112] C. Kunz, S. Engel, F.A. Müller, S. Gräf, Large-area fabrication of laser-induced periodic surface structures on fused silica using thin gold layers, Nanomaterial 10 (2020) 1187, https://doi.org/10.3390/NANO10061187, 2020, Vol. 10, Page 1187.
[113] B. Neuenschwander, B. Jaeggi, M. Schmid, G. Hennig, Surface structuring with ultra-short laser pulses: basics, limitations and needs for high throughput, Phys. Procedia 56 (2014) 1047–1058, https://doi.org/10.1016/J.PHPRO.2014.08.017.
[114] R. Zhou, Z. Zhang, M. Hong, The art of laser ablation in aeroengine: the crown jewel of modern industry, J. Appl. Phys. 127 (2020) 80902, https://doi.org/10.1063/1.5134813.
[115] A. De Zanet, V. Casalegno, M. Salvo, Laser surface texturing of ceramics and ceramic composite materials – A review, Ceram. Int. 47 (2021) 7307–7320, https://doi.org/10.1016/J.CERAMINT.2020.11.146.
[116] J. Martan, D. Moskal, L. Smeták, M. Honner, Performance and accuracy of the shifted laser surface texturing method, Micromachines 11 (2020) 520, https://doi.org/10.3390/mi11050520 (Basel).
[117] S. Mohammadi, H. Tavakoli-Anbaran, H. Zeinali, K. Obata, F. Caballero-Lucas, S. Kawabata, G. Miyaji, K. Sugioka, International journal of extreme manufacturing GHz bursts in MHz burst (BiBurst) enabling high-speed femtosecond laser ablation of silicon due to prevention of air ionization, IMMT Int. J. Extrem. Manuf. Int. J. Extrem. Manuf. 5 (2023) 7, https://doi.org/10.1088/2631-7990/acc0e5.
[118] K. Obata, F. Caballero-Lucas, S. Kawabata, G. Miyaji, K. Sugioka, GHz bursts in MHz burst (BiBurst) enabling high-speed femtosecond laser ablation of silicon due to prevention of air ionization, Int. J. Extrem. Manuf. 5 (2023), 025002, https://doi.org/10.1088/2631-7990/ACC0E5.
[119] D.R. Paschotta, Ultrafast lasers, Encycl. Laser Phys. Technol. (2008). https://www.rp-photonics.com/ultrafast_lasers.html (accessed August 22, 2022).
[120] W. Lin, T. Lai, Y. Cheng, X. Zheng, X. Xu, D. Mo, 60-fsec pulse generation from a self mode-locked Ti: sapphire laser, Guangxue Xuebao Acta Opt. Sin. 15 (1995) 1151–1152, https://doi.org/10.1364/ol.16.000042.
[121] B. Guo, J. Sun, Y. Hua, N. Zhan, J. Jia, K. Chu, Femtosecond laser micro/nano-manufacturing: theories, measurements, methods, and applications, Nanomanufacturing Metrol. 3 (2020) 26–67, https://doi.org/10.1007/s41871-020-00056-5.
[122] M. Martínez-Calderon, M. Manso-Silván, A. Rodríguez, M. Gómez-Aranzadi, J. P. García-Ruiz, S.M. Olaizola, R.J. Martín-Palma, Surface micro- and nano-texturing of stainless steel by femtosecond laser for the control of cell migration, Sci. Rep. 6 (2016) 1–10, https://doi.org/10.1038/srep36296, 2016 61.
[123] S.T. Hsu, H. Wang, G. Satoh, Y.L. Yao, Applications of surface structuring with lasers, in: Proceedings of the 30th International Congress on Applications of Lasers & Electro-Optics, ICALEO 2011, Laser Institute of America, 2011, pp. 1095–1104, https://doi.org/10.2351/1.5062186.
[124] K.H. Leitz, B. Redlingshöer, Y. Reg, A. Otto, M. Schmidt, Metal ablation with short and ultrashort laser pulses. Phys. Procedia, 2011, pp. 230–238, https://doi.org/10.1016/j.phpro.2011.03.128. Elsevier B.V.
[125] R. Indhu, V. Vivek, S. Loganathan, A. Bharatish, S. Soundarapandian, Overview of laser absorptivity measurement techniques for material processing, Lasers Manuf. Mater. Process. 5 (2018) 458–481, https://doi.org/10.1007/S40516-018-0075-1/FIGURES/19.
[126] G. Zhu, S. Wang, W. Cheng, G. Wang, W. Liu, Y. Ren, Investigation on the surface properties of 5A12 aluminum alloy after Nd: YAG laser cleaning, Coatings 9 (2019) 578, https://doi.org/10.3390/COATINGS9090578, 2019, Vol. 9, Page 578.
[127] L. Yang, Y. Ding, B. Cheng, J. He, G. Wang, Y. Wang, Investigations on femtosecond laser modified micro-textured surface with anti-friction property on bearing steel GCr15, Appl. Surf. Sci. 434 (2018) 831–842, https://doi.org/10.1016/J.APSUSC.2017.10.234.
[128] C. He, S. Yang, M. Zheng, Analysis of synergistic friction reduction effect on micro-textured cemented carbide surface by laser processing, Opt. Laser Technol. 155 (2022), 108343, https://doi.org/10.1016/J.OPTLASTEC.2022.108343.
[129] A.I. D. Brabazon, Laser Micro- and Nano-Scale Processing, IOP Publishing, London, 2021, https://doi.org/10.1088/978-0-7503-1683-5.
[130] T.H. Ting He, C.W. Chaoyang Wei, Z.J. Zhigang Jiang, Z.Y. Zhen Yu, Z.C. Zhen Cao, J.S. Jianda Shao, Numerical model and experimental demonstration of high precision ablation of pulse CO2 laser, Chin. Opt. Lett. 16 (2018), 041401, https://doi.org/10.3788/col201816.041401.
[131] P. Bartolo, J. Vasco, B. Silva, C. Galo, Laser micromachining for mould manufacturing: I. The influence of operating parameters, Assem. Autom. 26 (2006) 227–234, https://doi.org/10.1108/01445150610679777/FULL/PDF.
[132] T. Aizawa, T. Inohara, Pico- and femtosecond laser micromachining for surface texturing, in: Proceedings of the Micromachining, IntechOpen, 2019, https://doi.org/10.5772/intechopen.83741.
[133] A. Miotello, R. Kelly, Laser-induced phase explosion: new physical problems when a condensed phase approaches the thermodynamic critical temperature, Appl. Phys. A Mater. Sci. Process. 69 (1999) S67–S73, https://doi.org/10.1007/s003399900296.
[134] M. Mehrpouya, H. Lavvafi, A. Darafsheh, Microstructural Characterization and Mechanical Reliability of Laser-Machined Structures, Second Edi, Elsevier Ltd., 2018, https://doi.org/10.1016/b978-0-08-101252-9.00025-x.
[135] W. Fan, Y. Yang, R. Lou, X. Chen, J. Bai, W. Cao, G. Cheng, J. Si, Influence of energy fluence and overlapping rate of femtosecond laser on surface roughness of Ti-6Al-4V, Opt. Eng. 58 (2019) 1, https://doi.org/10.1117/1.oe.58.10.106107.
[136] F.H. Rajab, C.M. Liauw, P.S. Benson, L. Li, K.A. Whitehead, Production of hybrid macro/micro/nano surface structures on Ti6Al4V surfaces by picosecond laser surface texturing and their antifouling characteristics, Colloids Surf. B Biointerfaces 160 (2017) 688–696, https://doi.org/10.1016/J.COLSURFB.2017.10.008.
[137] S. Yang, K. Yin, J. Wu, Z. Wu, D. Chu, J. He, J.A. Duan, Ultrafast nano-structuring of superwetting Ti foam with robust antifouling and stability towards efficient oil-

in-water emulsion separation, Nanoscale 11 (2019) 17607–17614, https://doi.org/10.1039/C9NR04381K.
[138] J. Bonse, R. Koter, M. Hartelt, D. Spaltmann, S. Pentzien, S. Höhm, A. Rosenfeld, J. Krüger, Femtosecond laser-induced periodic surface structures on steel and titanium alloy for tribological applications, Appl. Phys. A Mater. Sci. Process. 117 (2014) 103–110, https://doi.org/10.1007/s00339-014-8229-2.
[139] S. Ye, Q. Cao, Q. Wang, T. Wang, Q. Peng, A highly efficient, stable, durable, and recyclable filter fabricated by femtosecond laser drilling of a titanium foil for oil-water separation, Sci. Rep. 6 (2016) 1–9, https://doi.org/10.1038/srep37591.
[140] C. Lanara, A. Mimidis, E. Stratakis, Femtosecond laser fabrication of stable hydrophilic and anti-corrosive steel surfaces, Materials 12 (2019) 3428, https://doi.org/10.3390/ma12203428 (Basel).
[141] M. Martínez-Calderon, A. Rodríguez, A. Dias-Ponte, M.C. Morant-Miñana, M. Gómez-Aranzadi, S.M. Olaizola, Femtosecond laser fabrication of highly hydrophobic stainless steel surface with hierarchical structures fabricated by combining ordered microstructures and LIPSS, Appl. Surf. Sci. 374 (2016) 81–89, https://doi.org/10.1016/J.APSUSC.2015.09.261.
[142] S.A. Jalil, M. Akram, J.A. Bhat, J.J. Hayes, S.C. Singh, M. ElKabbash, C. Guo, Creating superhydrophobic and antibacterial surfaces on gold by femtosecond laser pulses, Appl. Surf. Sci. 506 (2020), 144952, https://doi.org/10.1016/J.APSUSC.2019.144952.
[143] A.Y. Vorobyev, C. Guo, Multifunctional surfaces produced by femtosecond laser pulses, J. Appl. Phys. 117 (2015), 033103, https://doi.org/10.1063/1.4905616.
[144] H. Zhou, C. Li, Z. Zhou, R. Cao, Y. Chen, S. Zhang, G. Wang, S. Xiao, Z. Li, P. Xiao, Femtosecond laser-induced periodic surface microstructure on dental zirconia ceramic, Mater. Lett. 229 (2018) 74–77, https://doi.org/10.1016/J.MATLET.2018.06.059.
[145] J.H. Rakebrandt, Y. Zheng, H. Besser, T. Scharnweber, H.J. Seifert, W. Pfleging, Laser-assisted surface processing for functionalization of polymers on micro- and nano-scale, Microsyst. Technol. 26 (2019) 1085–1091, https://doi.org/10.1007/S00542-019-04633-7, 2019 264.
[146] Y. Assaf, A.M. Kietzig, Optical and chemical effects governing femtosecond laser-induced structure formation on polymer surfaces, Mater. Today Commun. 14 (2018) 169–179, https://doi.org/10.1016/J.MTCOMM.2018.01.008.
[147] E. Rebollar, J.R.V. de Aldana, I. Martín-Fabiani, M. Hernández, D.R. Rueda, T. A. Ezquerra, C. Domingo, P. Moreno, M. Castillejo, Assessment of femtosecond laser induced periodic surface structures on polymer films, Phys. Chem. Chem. Phys. 15 (2013) 11287–11298, https://doi.org/10.1039/C3CP51523K.
[148] F. Liang, J. Lehr, L. Danielczak, R. Leask, A.M. Kietzig, Robust non-wetting PTFE surfaces by femtosecond laser machining, Int. J. Mol. Sci. 15 (2014) 13681–13696, https://doi.org/10.3390/IJMS150813681, 2014, Vol. 15, Pages 13681-13696.
[149] B. Wang, X. Wang, H. Zheng, Y.C. Lam, Surface wettability modification of cyclic olefin polymer by direct femtosecond laser irradiation, Nanomaterial 5 (2015) 1442–1453, https://doi.org/10.3390/NANO5031442, 2015, Vol. 5, Pages 1442-1453.
[150] D. Chu, P. Yao, C. Huang, Anti-reflection silicon with self-cleaning processed by femtosecond laser, Opt. Laser Technol. 136 (2021), 106790, https://doi.org/10.1016/J.OPTLASTEC.2020.106790.
[151] Y. Cai, W. Chang, X. Luo, A.M.L. Sousa, K.H.A. Lau, Y. Qin, Superhydrophobic structures on 316L stainless steel surfaces machined by nanosecond pulsed laser, Precis. Eng. 52 (2018) 266–275, https://doi.org/10.1016/j.precisioneng.2018.01.004.
[152] S. Milles, M. Soldera, T. Kuntze, A.F. Lasagni, Characterization of self-cleaning properties on superhydrophobic aluminum surfaces fabricated by direct laser writing and direct laser interference patterning, Appl. Surf. Sci. 525 (2020), 146518, https://doi.org/10.1016/j.apsusc.2020.146518.
[153] D. Huerta-Murillo, A. García-Girón, J.M. Romano, J.T. Cardoso, F. Cordovilla, M. Walker, S.S. Dimov, J.L. Ocaña, Wettability modification of laser-fabricated hierarchical surface structures in Ti-6Al-4V titanium alloy, Appl. Surf. Sci. 463 (2019) 838–846, https://doi.org/10.1016/J.APSUSC.2018.09.012.
[154] A. Samanta, Q. Wang, S.K. Shaw, H. Ding, Nanostructuring of laser textured surface to achieve superhydrophobicity on engineering metal surface, J. Laser Appl. 31 (2019), 022515, https://doi.org/10.2351/1.5096148.
[155] Y.L. Sun, W.F. Dong, L.G. Niu, T. Jiang, D.X. Liu, L. Zhang, Y.S. Wang, Q.D. Chen, D.P. Kim, H.B. Sun, Protein-based soft micro-optics fabricated by femtosecond laser direct writing, Light Sci. Appl. 3 (2014), https://doi.org/10.1038/lsa.2014.10, 2014 31e129–e129.
[156] Y. Zabila, M. Perzanowski, A. Dobrowolska, M. Kac, A. Polit, M. Marszalek, Direct laser interference patterning: theory and application, Acta Phys. Pol. Ser. A 115 (2009) 591–593, https://doi.org/10.12693/APhysPolA.115.591.
[157] B. Voisiat, C. Zwahr, A.F. Lasagni, Growth of regular micro-pillar arrays on steel by polarization-controlled laser interference patterning, Appl. Surf. Sci. 471 (2019) 1065–1071, https://doi.org/10.1016/j.apsusc.2018.12.083.
[158] V. Lang, T. Roch, A.F. Lasagni, High-speed surface structuring of polycarbonate using direct laser interference patterning: toward 1 m2 min−1 fabrication speed barrier, Adv. Eng. Mater. 18 (2016) 1342–1348, https://doi.org/10.1002/adem.201600173.
[159] F. Schell, S. Alamri, T. Steege, C. Zwahr, T. Kunze, A. Lasagni, On the wetting behavior of laser-microtextured stainless steel using direct laser interference patterning, Surf. Coat. Technol. 447 (2022), 128869, https://doi.org/10.1016/J.SURFCOAT.2022.128869.
[160] S. Alamri, V. Vercillo, A.I. Aguilar-Morales, F. Schell, M. Wetterwald, A. F. Lasagni, E. Bonaccurso, T. Kunze, Self-limited ice formation and efficient de-icing on superhydrophobic micro-structured airfoils through direct laser interference patterning, Adv. Mater. Interfaces 7 (2020), https://doi.org/10.1002/ADMI.202001231.
[161] M. El-Khoury, B. Voisiat, T. Kunze, A.F. Lasagni, Utilizing a diffractive focus beam shaper to enhance pattern uniformity and process throughput during direct laser interference patterning, Material 15 (2022) 591, https://doi.org/10.3390/MA15020591, 2022, Vol. 15, Page 591.
[162] R. Baumann, S. Milles, B. Leupolt, S. Kleber, J. Dahms, F. Lasagni, Tailored wetting of copper using precise nanosecond direct laser interference patterning, Opt. Lasers Eng. 137 (2021), 106364, https://doi.org/10.1016/j.optlaseng.2020.106364.
[163] V. Vercillo, S. Tonnicchia, J.M. Romano, A. García-Girón, A.I. Aguilar-Morales, S. Alamri, S.S. Dimov, T. Kunze, A.F. Lasagni, E. Bonaccurso, Design rules for laser-treated icephobic metallic surfaces for aeronautic applications, Adv. Funct. Mater. 30 (2020), 1910268, https://doi.org/10.1002/adfm.201910268.
[164] A.I. Aguilar-Morales, S. Alamri, T. Kunze, A.F. Lasagni, Influence of processing parameters on surface texture homogeneity using direct laser interference patterning, Opt. Laser Technol. 107 (2018) 216–227, https://doi.org/10.1016/j.optlastec.2018.05.044.
[165] N. Schröder, F. Nyenhuis, R. Baumann, L. Mulko, T. Kiedrowski, J.A. L'huillier, A. F. Lasagni, Heating influence on hierarchical structures fabricated by direct laser interference patterning, Sci. Rep. 12 (2022) 1–10, https://doi.org/10.1038/s41598-022-22368-w, 2022 121.
[166] S. Alamri, M. El-Khoury, A.I. Aguilar-Morales, S. Storm, T. Kunze, A.F. Lasagni, Fabrication of inclined non-symmetrical periodic micro-structures using direct laser interference patterning, Sci. Rep. 2019 91. 9 (2019) 1–12. 10.1038/s41598-019-41902-x.
[167] A.H.A. Lutey, L. Gemini, L. Romoli, G. Lazzini, F. Fuso, M. Faucon, R. Kling, Towards laser-textured antibacterial surfaces, Sci. Rep. 8 (2018) 1–10, https://doi.org/10.1038/s41598-018-28454-2, 2018 81.
[168] O. Haim, J. Boger-Lombard, O. Katz, image-guided computational holographic wavefront shaping, (2023) 1–19. http://arxiv.org/abs/2305.12232.
[169] G.Z. Zhou, B. Chen, G. Wu, S. Qu, C.H. Chan, Arbitrary optical wavefront shaping with holographic plasmonic gap waveguides, Adv. Opt. Mater. 2300701 (2023) 1–9, https://doi.org/10.1002/adom.202300701.
[170] A.B. Ayoub, D. Psaltis, High speed, complex wavefront shaping using the digital micro-mirror device, Sci. Rep. 11 (2021) 1–10, https://doi.org/10.1038/s41598-021-98430-w.
[171] J. Sun, N. Koukourakis, J.W. Czarske, Complex wavefront shaping through a multi-core fiber, Appl. Sci. 11 (2021) 1–12, https://doi.org/10.3390/app11093949.
[172] Z. Kuang, W. Perrie, J. Leach, M. Sharp, S.P. Edwardson, M. Padgett, G. Dearden, K.G. Watkins, High throughput diffractive multi-beam femtosecond laser processing using a spatial light modulator, Appl. Surf. Sci. 255 (2008) 2284–2289, https://doi.org/10.1016/J.APSUSC.2008.07.091.
[173] R.J. Beck, J.P. Parry, W.N. Macpherson, A. Waddie, N.J. Weston, J.D. Shephard, D.P. Hand, R.R. Beck, J. Carrington, W. Parry, A. Macpherson, D.T. Waddie, N. Reid, J. Weston, D.P. Shephard, Application of cooled spatial light modulator for high power nanosecond laser micromachining, (2007).
[174] X. Sun, Z. Dong, K. Cheng, D. Chu, D. Kong, Y. Hu, J. Duan, Fabrication of oil–water separation copper filter by spatial light modulated femtosecond laser, J. Micromech. Microeng. 30 (2020), 065007, https://doi.org/10.1088/1361-6439/AB870D.
[175] G.L. Roth, S. Rung, C. Esen, R. Hellmann, Microchannels inside bulk PMMA generated by femtosecond laser using adaptive beam shaping, Opt. Express 28 (2020), https://doi.org/10.1364/OE.384948.
[176] E.G. Gamaly, A.V. Rode, B. Luther-Davies, V.T. Tikhonchuk, Ablation of solids by femtosecond lasers: ablation mechanism and ablation thresholds for metals and dielectrics, Phys. Plasmas 9 (2002) 949, https://doi.org/10.1063/1.1447555.
[177] Y.T. Cheng, D.E. Rodak, C.A. Wong, C.A. Hayden, Effects of micro- and nano-structures on the self-cleaning behaviour of lotus leaves, Nanotechnology 17 (2006) 1359–1362, https://doi.org/10.1088/0957-4484/17/5/032.
[178] M.I. Kayes, A.J. Galante, N.A. Stella, S. Haghanifar, R.M.Q. Shanks, P.W. Leu, Stable lotus leaf-inspired hierarchical, fluorinated polypropylene surfaces for reduced bacterial adhesion, React. Funct. Polym. 128 (2018) 40–46, https://doi.org/10.1016/j.reactfunctpolym.2018.04.013.
[179] G.S. Watson, D.W. Green, L. Schwarzkopf, X. Li, B.W. Cribb, S. Myhra, J. A. Watson, A gecko skin micro/nano structure - A low adhesion, superhydrophobic, anti-wetting, self-cleaning, biocompatible, antibacterial surface, Acta Biomater. 21 (2015) 109–122, https://doi.org/10.1016/j.actbio.2015.03.007.
[180] E.P. Ivanova, J. Hasan, H.K. Webb, V.K. Truong, G.S. Watson, J.A. Watson, V. A. Baulin, S. Pogodin, J.Y. Wang, M.J. Tobin, C. Löbbe, R.J. Crawford, Natural bactericidal surfaces: mechanical rupture of pseudomonas aeruginosa cells by cicada wings, Small 8 (2012) 2489–2494, https://doi.org/10.1002/smll.201200528.
[181] D.W. Bechert, M. Bruse, W. Hage, Experiments with three-dimensional riblets as an idealized model of shark skin, Exp. Fluids 28 (2000) 403–412, https://doi.org/10.1007/s003480050400.
[182] M.D. Ibrahim, S.N.A. Amran, A. Zulkharnain, Y. Sunami, Streamlined vessels for speedboats: macro modifications of shark skin design applications, in: Proceedings of the AIP Conference Proceedings, American Institute of Physics Inc., 2018, 101510, https://doi.org/10.1063/1.5021936.
[183] X.Q. Bai, G.T. Xie, H. Fan, Z.X. Peng, C.Q. Yuan, X.P. Yan, Study on biomimetic preparation of shell surface microstructure for ship antifouling, Wear 306 (2012) 285–295, https://doi.org/10.1016/j.wear.2012.11.020.

[184] A.M. Brzozowska, F.J. Parra-Velandia, R. Quintana, Z. Xiaoying, S.S.C. Lee, L. Chin-Sing, D. Jańczewski, S.L.M. Teo, J.G. Vancso, Biomimicking micropatterned surfaces and their effect on marine biofouling, Langmuir 30 (2014) 9165–9175, https://doi.org/10.1021/LA502006S/SUPPL_FILE/LA502006S_SI_002.PDF.

[185] K. Sun, H. Yang, W. Xue, A. He, D. Zhu, W. Liu, K. Adeyemi, Y. Cao, Anti-biofouling superhydrophobic surface fabricated by picosecond laser texturing of stainless steel, Appl. Surf. Sci. 436 (2018) 263–267, https://doi.org/10.1016/j.apsusc.2017.12.012.

[186] Y. Tuo, H. Zhang, L. Chen, W. Chen, X. Liu, K. Song, Fabrication of superamphiphobic surface with hierarchical structures on metal substrate, Colloids Surf. A Physicochem. Eng. Asp. (2021) 612, https://doi.org/10.1016/J.COLSURFA.2020.125983.

[187] L. Wang, Q.D. Chen, X.W. Cao, R. Buividas, X. Wang, S. Juodkazis, H.B. Sun, Plasmonic nano-printing: large-area nanoscale energy deposition for efficient surface texturing, Light Sci. Appl. 6 (2017), https://doi.org/10.1038/lsa.2017.112 e17112–e17112.

[188] J. Bonse, S. Gräf, Maxwell meets Marangoni—A review of theories on laser-induced periodic surface structures, Laser Photon. Rev. 14 (2020), 2000215, https://doi.org/10.1002/lpor.202000215.

[189] J.E. Sipe, J.F. Young, J.S. Preston, H.M. van Driel, Laser-induced periodic surface structure. I. Theory, Phys. Rev. B 27 (1983) 1141–1154, https://doi.org/10.1103/PhysRevB.27.1141.

[190] G. Giannuzzi, C. Gaudiuso, R. Di Mundo, L. Mirenghi, F. Fraggelakis, R. Kling, P. M. Lugarà, A. Ancona, Short and long term surface chemistry and wetting behaviour of stainless steel with 1D and 2D periodic structures induced by bursts of femtosecond laser pulses, Appl. Surf. Sci. 494 (2019) 1055–1065, https://doi.org/10.1016/j.apsusc.2019.07.126.

[191] N. Epperlein, F. Menzel, K. Schwibbert, R. Koter, J. Bonse, J. Sameith, J. Krüger, J. Toepel, Influence of femtosecond laser produced nanostructures on biofilm growth on steel, Appl. Surf. Sci. 418 (2017) 420–424, https://doi.org/10.1016/J.APSUSC.2017.02.174.

[192] P. Ares, K.S. Novoselov, Recent advances in graphene and other 2D materials, Nano Mater. Sci. 4 (2022) 3–9, https://doi.org/10.1016/j.nanoms.2021.05.002.

[193] C.D. Powell, L. Pisharody, J. Jopp, R. Sharon-Gojman, B.A. Tesfahunegn, C. J. Arnusch, Laser-induced graphene capacitive killing of bacteria, ACS Appl. Bio Mater. 6 (2023) 883–890, https://doi.org/10.1021/ACSABM.2C01034.

[194] E. Manderfeld, M.N. Kleinberg, C. Thamaraiselvan, F. Koschitzki, P. Gnutt, N. Plumere, C.J. Arnusch, A. Rosenhahn, Electrochemically activated laser-induced graphene coatings against marine biofouling, (2021). 10.1016/j.apsusc.2021.150853.

[195] S. Beikzadeh, A. Akbarinejad, J. Taylor, S. Swift, D. Simonov, J. Ross, J. Perera, P. A. Kilmartin, J. Travas-Sejdic, Charged laser-induced graphene electrodes exhibit strong capacitance-based antibacterial and antiviral properties, (2023). 10.1016/j.apmt.2023.101753.

[196] N.H. Barbhuiya, A. Kumar, S.P. Singh, A journey of laser-induced graphene in water treatment, Trans. Indian Natl. Acad. Eng. 6 (2021) 159–171, https://doi.org/10.1007/s41403-021-00205-2.

[197] Q. Zhang, F. Zhang, X. Liu, Z. Yue, X. Chen, Z. Wan, Doping of laser-induced graphene and its applications, Adv. Mater. Technol. (2023), https://doi.org/10.1002/ADMT.202300244.

[198] M. Ebrahimi, M. Asadi, O. Akhavan, Graphene-based nanomaterials in fighting the most challenging viruses and immunogenic disorders, ACS Biomater. Sci. Eng. 8 (2022) 54–81, https://doi.org/10.1021/acsbiomaterials.1c01184.

[199] J. Lin, Z. Peng, Y. Liu, F. Ruiz-Zepeda, R. Ye, E.L.G. Samuel, M.J. Yacaman, B. I. Yakobson, J.M. Tour, Laser-induced porous graphene films from commercial polymers, Nat. Commun. 5 (2014) 1–8, https://doi.org/10.1038/ncomms6714.

[200] S. Liu, T.H. Zeng, M. Hofmann, E. Burcombe, J. Wei, R. Jiang, J. Kong, Y. Chen, Antibacterial activity of graphite, graphite oxide, graphene oxide, and reduced graphene oxide: membrane and oxidative stress, ACS Nano 5 (2011) 6971–6980, https://doi.org/10.1021/nn202451x.

[201] A.K. Thakur, S.P. Singh, C. Thamaraiselvan, M.N. Kleinberg, C.J. Arnusch, Graphene oxide on laser-induced graphene filters for antifouling, electrically conductive ultrafiltration membranes, J. Memb. Sci. 591 (2019), 117322, https://doi.org/10.1016/j.memsci.2019.117322.

[202] H. Jin, L. Tian, W. Bing, J. Zhao, L. Ren, Bioinspired marine antifouling coatings: status, prospects, and future, Prog. Mater. Sci. 124 (2022), https://doi.org/10.1016/J.PMATSCI.2021.100889.

[203] J. Chapman, F. Regan, Nanofunctionalized superhydrophobic antifouling coatings for environmental sensor applications—Advancing deployment with answers from nature, Adv. Eng. Mater. 14 (2012) B175–B184, https://doi.org/10.1002/ADEM.201180037.

[204] C. Richards, A. Slaimi, N.E. O'connor, A. Barrett, S. Kwiatkowska, F. Regan, Bio-inspired surface texture modification as a viable feature of future aquatic antifouling strategies: a review, Int. J. Mol. Sci. 21 (2020) 1–20, https://doi.org/10.3390/ijms21145063.

[205] A. Abbott, P.D. Abel, D.W. Arnold, A. Milne, Cost–benefit analysis of the use of TBT: the case for a treatment approach, Sci. Total Environ. 258 (2000) 5–19, https://doi.org/10.1016/S0048-9697(00)00505-2.